Electronics & Computer Science
Faculty of Physical Science & Engineering
University of Southampton

By James Howe

May 10, 2021

Electroencephalographic [EEG] Control of Robotics

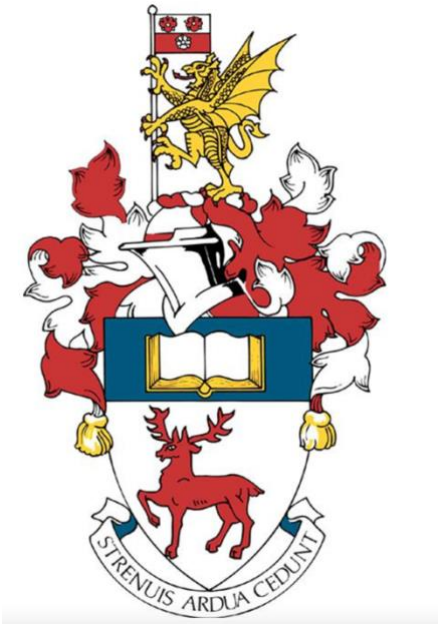

Project supervisor: Dr Tracy Melvin
Second examiner: Dr Abhinav Kumar Singh

A project report submitted for the award of
BEng Mechatronics Engineering

Abstract

In order to explore the potential for applying biological signals, notably neurological signals in the cortex of the brain, for the control of mechanical/robotic systems an electroencephalogram or EEG is to be built. It is well established that different cortical regions are stimulated for discrete human functions, notably for motor control, visual functions, as well as other sensory functions. The cortical regions for different functions will be investigated and then the electroencephalogram [EEG] will be tested to establish the optimum location of the electrodes on the brain for signals that can be used as switches for various control functions of a robotic system.

Statement of Originality

- I have read and understood the ECS Academic Integrity information and the University's Academic Integrity Guidance for Students.
- I am aware that failure to act in accordance with the Regulations Governing Academic Integrity may lead to the imposition of penalties which, for the most serious cases, may include termination of programme.
- I consent to the University copying and distributing any or all of my work in any form and using third parties (who may be based outside the EU/EEA) to verify whether my work contains plagiarised material, and for quality assurance purposes.

You must change the statements in the boxes if you do not agree with them.

We expect you to acknowledge all sources of information (e.g. ideas, algorithms, data) using citations. You must also put quotation marks around any sections of text that you have copied without paraphrasing. If any figures or tables have been taken or modified from another source, you must explain this in the caption and cite the original source.

I have acknowledged all sources, and identified any content taken from elsewhere.

If you have used any code (e.g. open-source code), reference designs, or similar resources that have been produced by anyone else, you must list them in the box below. In the report, you must explain what was used and how it relates to the work you have done.

Original circuit design from Instructables user cah6. Citations appropriately with significant changes made by myself.

You can consult with module teaching staff/demonstrators, but you should not show anyone else your work (this includes uploading your work to publicly-accessible repositories e.g. Github, unless expressly permitted by the module leader), or help them to do theirs. For individual assignments, we expect you to work on your own. For group assignments, we expect that you work only with your allocated group. You must get permission in writing from the module teaching staff before you seek outside assistance, e.g. a proofreading service, and declare it here.

I did all the work myself, or with my allocated group, and have not helped anyone else.

We expect that you have not fabricated, modified or distorted any data, evidence, references, experimental results, or other material used or presented in the report. You must clearly describe your experiments and how the results were obtained, and include all data, source code and/or designs (either in the report, or submitted as a separate file) so that your results could be reproduced.

The material in the report is genuine, and I have included all my data/code/designs.

We expect that you have not previously submitted any part of this work for another assessment. You must get permission in writing from the module teaching staff before re-using any of your previously submitted work for this assessment.

I have not submitted any part of this work for another assessment.

If your work involved research/studies (including surveys) on human participants, their cells or data, or on animals, you must have been granted ethical approval before the work was carried out, and any experiments must have followed these requirements. You must give details of this in the report, and list the ethical approval reference number(s) in the box below.

My work did not involve human participants, their cells or data, or animals.

ECS Statement of Originality Template, updated August 2018, Alex Weddell
aiofficer@ecs.soton.ac.uk

Acknowledgements

I would like to thank Dr Tracy Melvin for her consistent and extremely useful advice throughout the year. Her guidance has made what is the largest project I've completed to date more enjoyable and interesting, allowing me to create something of which I can be proud.

I would also like to thank the lab technicians for their help with technical issues on a much-reduced time scale. With their help I was able to make the most of the lab time left available.

It is with sorrow and joy I would also like to thank Dr Mike Hogg of the foundation year lecturing staff. As many of the foundation year students that come before me will agree, he was and remains one of a kind. His presence, character and unique charm on campus will be sorely missed.

Content

List of Figures

List of Tables

Chapter 1: Project Description

The project looks at isolating the neurological signals within the brain, specifically the motor cortex to distinguish regions of specific control. Most current research focuses on using the magnitude of general brain activity within a given area for control of a system. This project will explore the potential for an increase in accuracy of this control by exploiting and breaking down the motor cortex into its constituents so that many, more responsive 'switches' could be implemented into a robotic system.

To demonstrate this a switch control system will be explored using only activation of the muscles in the arms. This will involve research into the literature of the brain, assessing if a system could distinguish between the different regions using electrodes in an array of locations along the motor cortex.

The report describes the engineering components needed to create an electroencephalogram. The background research establishes the biological phenomena that allows for electronics to take readings. The process and requirements needed to design and build a system is posed and then built to show it plausibility.

Chapter 2: Introduction

Problem

This project is proposed with the potential for transferable applications to the health sector. Such research is key to improving the quality of life for patients struggling with mobility-based disabilities (i.e., paraplegic patients, stroke patients). The integration of robotic tools with neurological processes in the brain requires the use of tools such as Electroencephalographic (EEG) headset. Such tools have been demonstrated for computer games as well as for tools for disabled people to perform simple tasks. *(Fok et all, 2011 [29]) (Nasreddine et all, 2015 [30])*

Goals

The Goal is to explore the feasibility and practicality of controlling a simple robotic system using an Electroencephalographic (EEG) headset. This will be achieved by identification of specific regions of the brain to be used for control purposes. Once this region has been identified, electrodes can be placed on the scalp in appropriate regions for 'signature' signals to be identified. This data will then be amplified, modulated and later used for control of a robot. *(Meng et all, Dec 2016 [31]).*

Scope

- *Biological elements*

Given this system is based entirely on exploiting the electrochemical response within the brain's neurons. In order to usefully understand and innovate in this area a decent level of understanding into the underlying biological elements will need to be explored first.

- *Electroencephalographic (EEG) headset*

In order to construction an EEG headset the current technology harnessed and modified in order to achieve the project goals. A device will be constructed for the project which will include hardware filters to isolate the frequency of the useful data that is to be applied for control of an electromechanical systems.

- *Control software*

Initially the software associated with the project was to be used so that the system could be self-contained and have easy repurposing of the output switches from the EEG to different robotic systems. Software was written to cycle through the electrodes of the system to be fed into the EEG.

- *Robot for control*

The initial aim was to control a robot with an emphasis on the transferable applications towards the health sector. A potential idea would be to explore the use of using an EEG to control a simple commercially available remote-controlled car as the idea could be transferred to control of an electric wheelchair.

Chapter 3: Background research

The brain's function can be likened to the central processing unit (CPU) of a computer. It takes inputs from various senses around the body including touch, taste, sight, hearing, smell and internal sensing which sends signals to the brain via the spinal cord through the use of neurons. The sensory input can be applied for motor signals for mobility and movement. For patients with mobility-based disabilities the signals in the motor cortical regions can be detected by electrodes that are strategically positioned over the motor cortex and applied as a signal for electrical control of a robotic system, or even to control a computer game. (Belkacem et al., 2015, [4])

3.1. The Neuron

There are approximately 86 billion neurons in a human brain. Neurons are the 'communication systems' and are responsible for 'sending and receiving signals' from all parts of the brain, spinal cord and sensory cells found within the body.

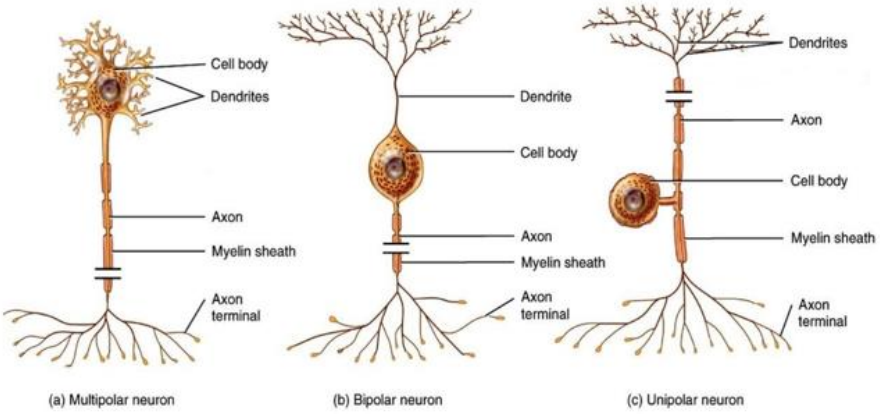

(Biga et all., 2002, [5]) [Figure 3.1.1: Three distinct variations in the neurons purpose and structure. Categorized as the following]

Afferent neurons send ‘signals’ from the sensory receptors triggered by the environment, corresponding to all five senses (touch, taste, vision, hearing, taste). These ‘signals’ are sent toward the central nervous system (CNS). The neurons are unipolar or pseudo-unipolar in nature meaning the cell body is placed adjacent to the length of the axon via a single connection allowing for faster transmission to the spinal cord terminal. The axons in unipolar sensory neurons can “reach about 5ft”, making them the longest from of neuron. (Jennes, 2017, [13])

Efferent neurons send ‘signals’ from the central nervous system to the spinal cord for motor function. These neurons are multipolar and have a length in the range 100-130µm. (Kovac, 2018, [15]) These neurons are responsible for stimulation of muscle tissue.

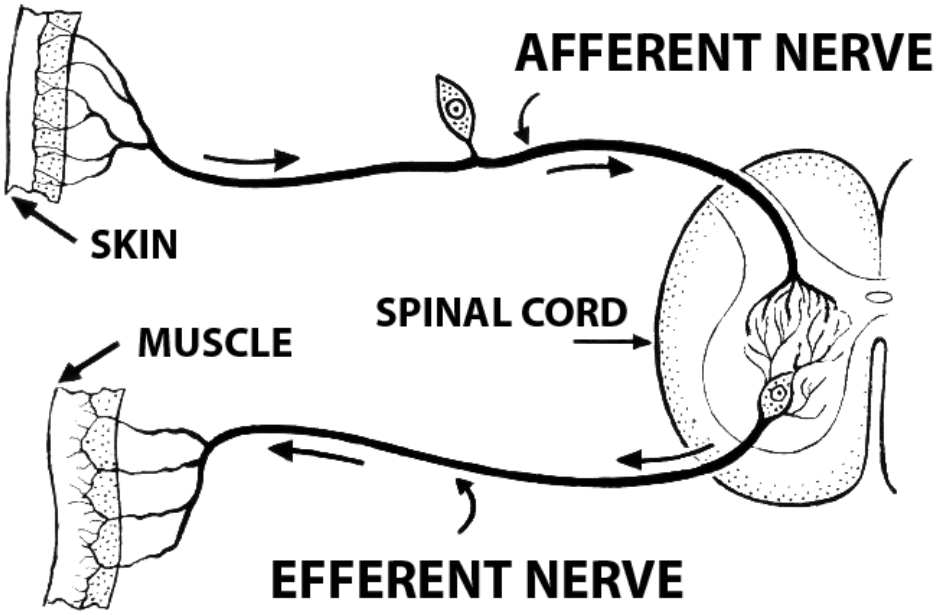

(The Albert Team, 2020, [27]) [Figure 3.1.2: Afferent and Efferent nerve (neuron) pathway with interneurons along spinal cord]

Interneurons or associative neurons are present within the central nervous system and spinal cord to connect the sensory and motor neurons. They are mostly unipolar neurons though much shorter than motor neurons at approximately 5µm. (Kavoc, 2018, [15])

Forming a tree-like structure, dendrites are responsible for receiving ‘transmission information’ from nearby axon terminals. In the case of motor (multipolar) neurons, they extend roots outward from the Perikarya which surrounds and contains the cell nucleus.

The axon propagates the ‘signals’ through the process of action potentials. Axons are narrow chord structures with a radius around 0.5-10µm which remains relatively constant in size along the length. Some axons are protected by a layer of Schwann cells called the Myelin Sheath, this sheath facilities transmission of the ‘signal’ along the axon to the synapse. Myelination can be likened to ‘electrical insulation’ and is the result of oligodendrocytes around the axon. Unlike Schwann cells which wrap around the whole cell body and axon, these cells in the CAN lack the regular partition Node of Ranvier which are seen in the peripheral nervous system. (Jennes, 2017, [13])

The brain has approximately 100 billion neurons each with between 1000 – 10000 synapses, making a total of around 100 – 1000 trillion synapse connections in the brain. The synaptic

junctions are the interface between two or more different neurons. There are two variations in the process behind the transmission of the 'signal' over the synapse which can change over time. Electrical synapses are much more abundant in the embryonic nervous tissue where they help guide neural development. As the nervous system matures some of these electrical synapses can be replaced with chemical (neurotransmitter) equivalents. The electrical synapses, though able to propagate much faster, are less precise than their chemical counterpart.

In order for 'signals' to be transferred along neuronal axons an event must occur which triggers an 'all or nothing' response within the neuron.

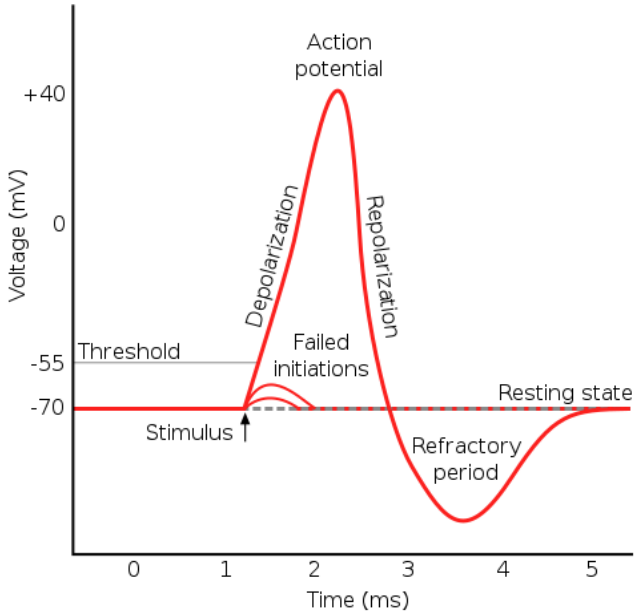

(Khanna, 2020, [14]) [Figure 3.1.3: Voltage vs Time breakdown of the stages of action potential within a neuron]

With the neuron, at resting state there is a potential difference across the membrane of approximately 70mV. Stimulation is initiated at the dendrites, propagating through the Perikarya to the axon hillock. "The axon hillock is a highly specialised area in the perikaryon devoid of most organelles; however, its plasma membrane contains a very high density of voltage-gated ion channels that are needed to initiate an action potential". If the synaptic potential of the stimulus is below the threshold voltage of 55mV then a graded potential will occur, and the neuron will quickly return to resting potential. (Jennes, 2017, [13])

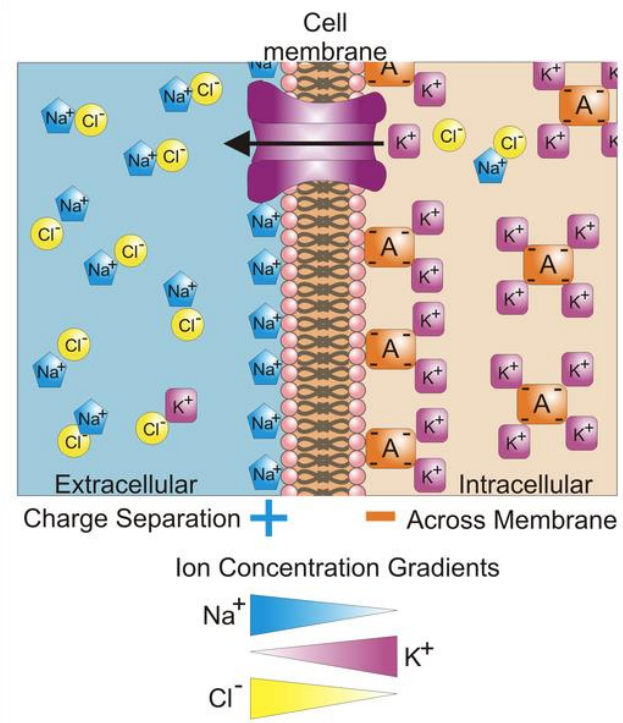

(Khanna, 2020, [14]) [Figure 3.1.4: Distribution of positive and negative chemical ions inside and outside of the axon of a neuron]

If however the stimulus is in excess of this threshold potential then the process of depolarization will take place. All along the axon, inside the membrane that surrounds it are gated channels which allows the charged anions and cations inside or outside the membrane wall to pass through, thus altering the net potential across the cell wall. Depolarization begins when the stimulus reaches the axon hillock. The sodium ions enter the axon, increasing the net potential to +40mV. The result of this excitation is a brief reversal of the potential at a specific point along the membrane of the axon. It is this reversal in potential that propagates unidirectionally toward the synapses as the reaction repeats.

In order for Repolarization to take hold, voltage gated potassium channels are opened allowing ions to move from the intercellular to the extracellular region. This attempts to rebalance the charges along the membrane.

As a result of the repolarization and voltage gated potassium channels opening, hyperpolarization takes place to prevent propagation in the wrong direction. This happens when too many potassium ions are moved into the extracellular region thus creating a charge lower than the resting potential as seen in figures 3.1.3 & 3.1.4.

Finally, during the refractory period sodium-potassium pumps are used to resort the chemicals to their side of origin. After this process the neuron will have returned to its resting state as the action potential propagates down the axon repeating this process.

3.2. Anatomy of the Brain

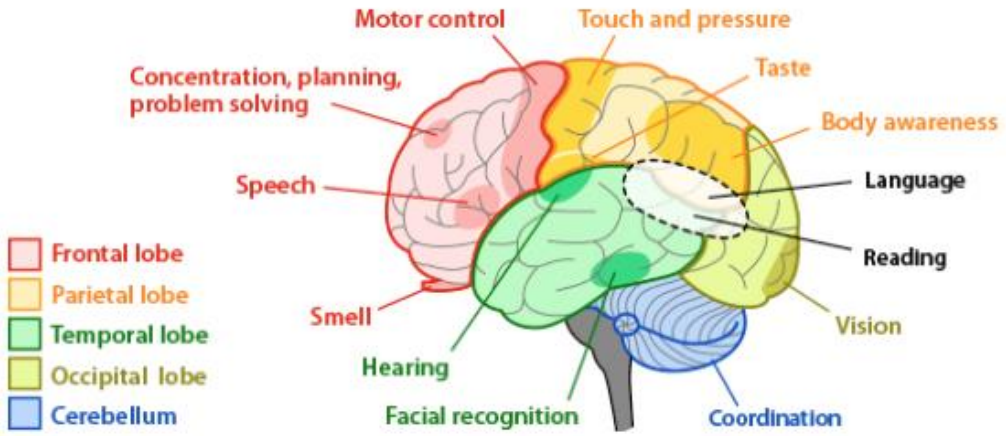

(Szymik, May 9, 2011, [25]) [Figure 3.2.1: Locations of lobes in cortical and cerebellum regions and the associated functions]

As shown in figure 3.2.1, the various lobes of the cortex have been mapped to different neurological functions, the neocortex, which is the outer surface of the cortex is built up of Sulci, which are the folds of the brain tissue in the cortical interfaces, and this allows for greater numbers of neuronal connections and also organisation due to the increased surface area it creates.

The two 'hemispheres' of the brain, communicate with one another through the use of nerve fibres called the Corpus Collosum. The left and right hemispheres provide motor and sensory control of the right and left side respectively. The cerebrum is also responsible for vision, language, hearing, taste, as shown in figure 3.2.1.

The Occipital cortex is where visual processing takes place and memory recall tasks associated with specific imagery are processed.

Responsible for what is described as "executive function and cognitive control", the Frontal cortex encompasses fundamentals of our consciousness including a working memory, cognitive inhibition, cognitive flexibility and our attention span. (Davidson et al., 2006, [10])

The temporal lobe is responsible for processing language, written and spoken information.

Used for consolidating all the information sent from the body, the parietal lobe gives us reference to the environment in close proximity. Direct interactions with the local environment heavily incorporate this region of the brain for tasks like eye-tracking and hand-eye coordination. With the use of both eyes, the occipital lobe and parietal lobe the concept of depth perception is possible, giving accurate interaction with nearby objects.

The cerebellum works to regulate 'signals' from the spinal cord to the associated region of the brain for processing. There are however operations associated with the 'little brain' Including, but not limited to motor learning, balance, coordination and posture. Represented in grey below the cerebellum in Figure 3.2.1 the Stem connects the spinal cord and the brain. It is also associated with some internal reflex controls including regulating our breathing, heart rate, swallowing, temperature and more. Both the cerebellum and the stem are located too far inside

the skull for measurements to be taken using electroencephalography so will not be considered for control.

3.3. The Cortical Regions

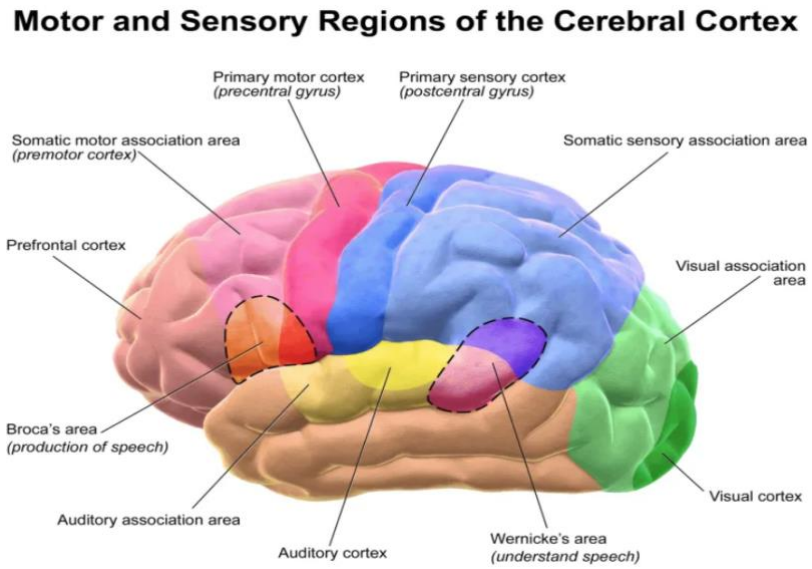

(The Human Memory, 2020, [12]) [Figure 3.3.1: Motor, Sensory and Associative regions of the brain]

The cortical regions, located in the Neocortex are attributed with sensory, motor and associative functions. The Thalamus (located above the stem) sends sensory and motor information to the appropriate region for processing. The five senses available to us each have a specific associated area of the cortical region that categorizes and integrates information.

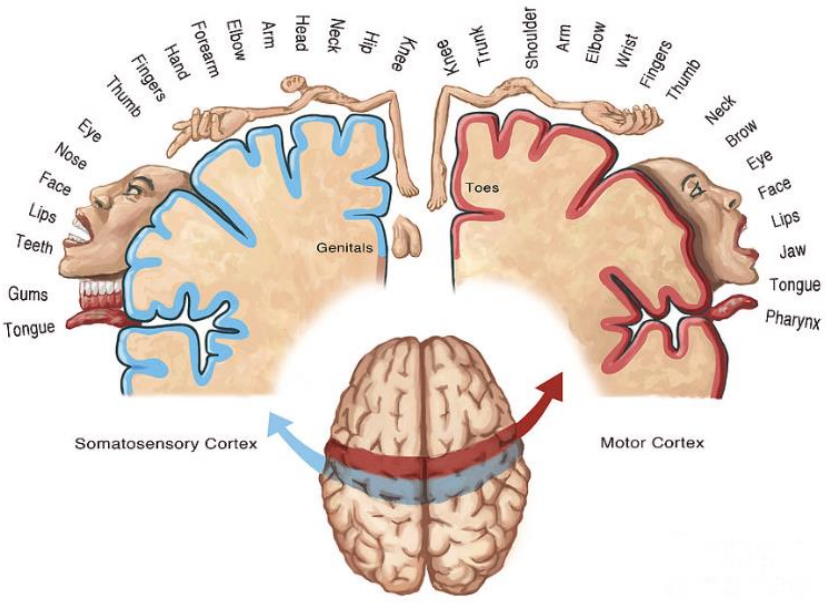

(Sutton, 2018, [24]) [Figure 3.3.2: The Homunculus Map showing the Sensory and Motor cortex and the associated affected region of the body for efferent or afferent response. Used for initial locations of electrode placement]

The main parts of the sensory area include the auditory cortex, the somatosensory cortex (primary sensory cortex) and the visual cortex. The aspects of the body receiving and

processing sensory information are located in the somatosensory cortex which is directly behind the somatomotor cortex with the same control locations. Some areas of the body however don't have a reflected area in the motor cortex as only afferent nerves are present (for example teeth and gums) This allows for efficient, fast reaction times given the proximity between sensory and motor regions of the cortical regions.

The motor regions are built up of the somatomotor cortex (primary motor cortex), the somatic motor association area which contains the premotor cortex and the posterior parietal cortex (located in a small region directly behind the top of the primary somatosensory cortex).

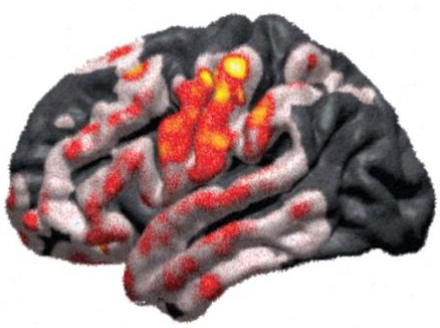

(Bundy et al., 2018, [7]) (Azvolinsky, 2018, [3]) [Figure 3.3.3: Dual hemisphere response from stimulating movement in one arm. Artistic/academic imaging of the active motor cortex]

The primary motor cortex is responsible for the planned movement of the body. The somatic motor association and premotor cortex are responsible for planning of sequential movement, like walking.

The associative regions include the Wernicke's and Broca's areas which are used in producing and understanding speech, prefrontal association area involved in motor planning and abstract thought. The main purpose of these areas is to link signals from sensory information in the present with past experiences. For a task repeated many times, long term muscle memory can be enhanced resulting in an efficient and accurate motor response.

3.4. Measurements of Electrical Activity in the Brain – Pyramidal Cells

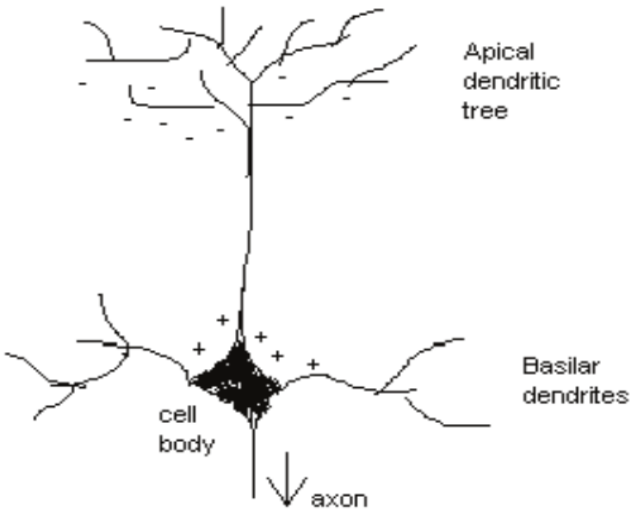

(Salvetti & Wilamowski, 2008, [20]) [Figure 3.4.1: Diagram of a Pyramidal cell (neuron) at resting state and the key regions]

Only impulses located on the top surface of the neocortex can be accurately received by the electrode of an encephalogram. These readings are possible through the exploitation of pyramidal cells. These pyramidal neurons (which are bipolar in nature) are organised parallel to one another, and perpendicular to the surface of the cerebral cortex.

The currents produced outside of most neuronal cells by action potentials along the axon generally result in a net zero current given the relatively random set of orientations. The pyramidal cells are different, mainly due to the fact that they are aligned and oriented with the surface of the neocortex. Neurotransmitters move from the synapse to the post-synaptic membrane. This, similar to the action potential process causes ion channels to open allowing +ve ions to flow into the cell resulting in a net negative charge around the cell body (sink). The positive flow of ions eventually leaves via the apical dendrites which results in the extracellular space becoming positively charged (source). This reversal of polarity propagates along to other pyramidal cells as the impulse is transmitted through the brain.

The pyramidal cells can be found in abundance along the surface of the cerebrum. When a task is being carried out a large number of them are active at once, so the reading is a summation of these potentials related to a specific motor function as a precise location. Difficulties arise given that motor functions are not distinct in location. One region can be associated with a multitude of similar tasks.

A simple system for electrode placement can be found in the 10-20 positioning though this will only be used as a rough guide when referring to general areas.

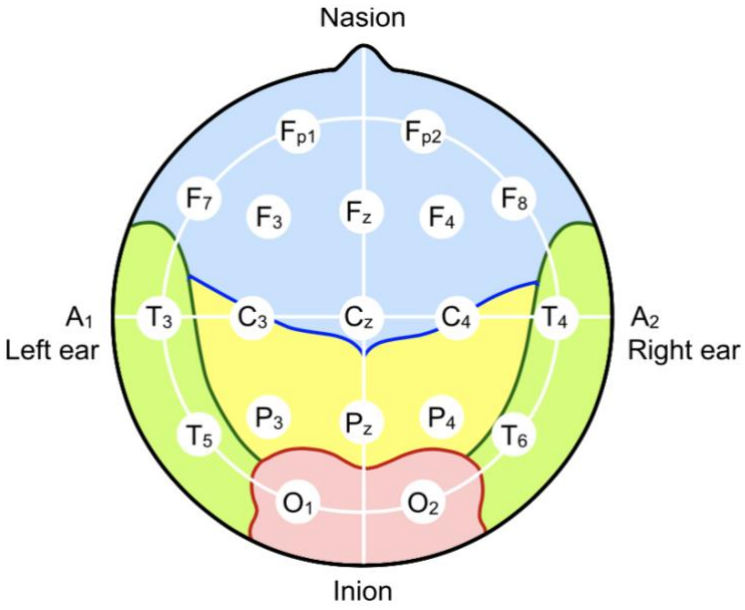

(Bos, 2006, [3]) [Figure 3.4.2: 10-20 system for electrode placement on the scale for shorthand notation of locations]

3.5. History of EEG in Rehabilitation and Diagnostics

EEG was first used by neurosurgeon Nikolai Guleke in 1924. Han Berger expanded upon discoveries made by others including Caton and Beck. For the first 20 years EEG has been used as a tool within the medical rehabilitation technologies. (Stone & Hughes, 2013, [23])

Epilepsy

The first clinical application for EEG was for Epilepsy, notably its use in recording brain activity during a seizure (Reif et al., 2016, [19])

(Stefen et al., 2012, [23]) [Figure 3.5.1: Epilepsy case study with electrodes placed using the 10-20 placement systems for detection of the region of origin of a given seizure]

EEG is used to rank and categorize the severity of the Epilepsy within a patient, helping doctors determine what antiepileptics to prescribe. "EEG findings contribute to the multi-axial diagnosis of epilepsy, in terms of whether the seizure disorder is focal or generalised, idiopathic or symptomatic, or part of a specific epilepsy syndrome." (Smith, 2005, [22])

Constituting about 5% of epilepsy patients, photosensitive epilepsy patients could be diagnosed by subjecting them to flashing lights at different frequencies in a controlled environment to see if it triggers a seizure response. This diagnosis can be key to avoiding such triggers in everyday life. (Smith, 2005, [22])

REM Sleep

EEG is the preferred tool for analysing sleep within the research field. This is done by identification of the waveforms associated with each stage of the sleep cycle, notably Rapid Eye Movement (REM) and NON-REM (NREM), which typically occurs in cycles over the course of a night. Factors that can alter the reading include the quality and quantity of sleep in the nights prior to testing, drugs administered, legal or otherwise. Results expected in each stage can be shown in figure 3.5.2. (Campbell, 2019, [9])

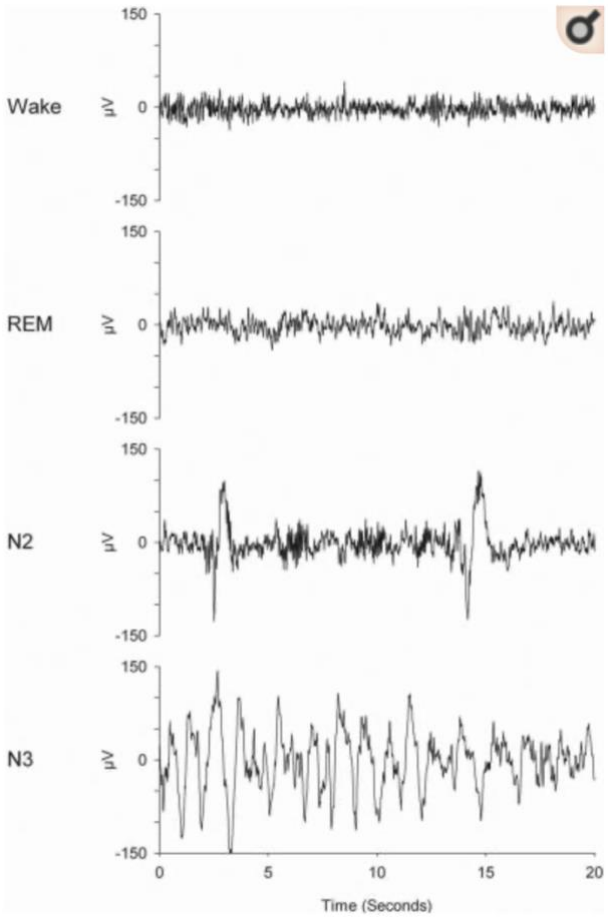

(Campbell, 2019, [9]) [Figure 3.5.2: Shows the amplitudes and frequencies in a 21yr old over a 20 second period. N2 is the period between REM and NREM, N3 is in NREM]

BCI Control System

In recent years the use of EEG systems has been exploited by those making prosthetics. Specifically, EEG is being used as a non-invasive BCI (brain-computer interface) where, by reading the impulses in the cortical region associated with a given group of muscles a control system can be implemented. In other research the control is based on the intensity of the user's concentration to control switches, though this has a reduced level of accuracy. This method is low cost, low intrusion when compared to some of the existing methods of BCI control and also more intuitive after a training period. (Bright et al., 2016, [6])

Applying this technology to not only patients in rehabilitation but also those who's motor function is completely lost. Spinal cord injuries and brainstem stoke patients could utilize a BCI control system shown in Figure 3.5.3 and those with amyotrophic lateral sclerosis could be privy to a BCI communication system. Those with some remaining motor control could be beneficiaries of a BCI mobility system as shown in Figure 3.5.4. (Machado et al., 2010, [16])

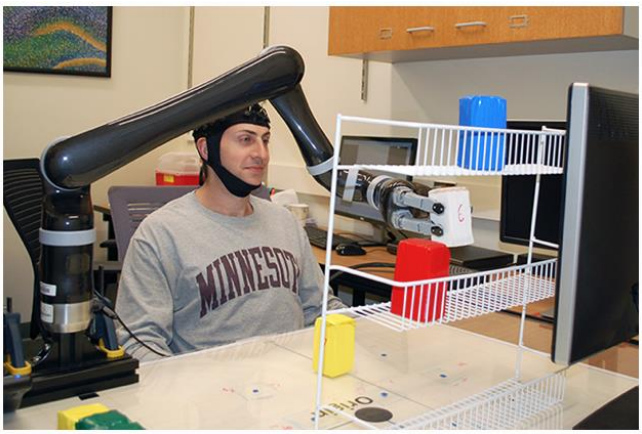

(Mok, 2017, [18]) [Figure 3.5.3: Review article on EEG BCI system from the University of Minnesota controlling an independent robotic arm with a testing success rate of 70%]

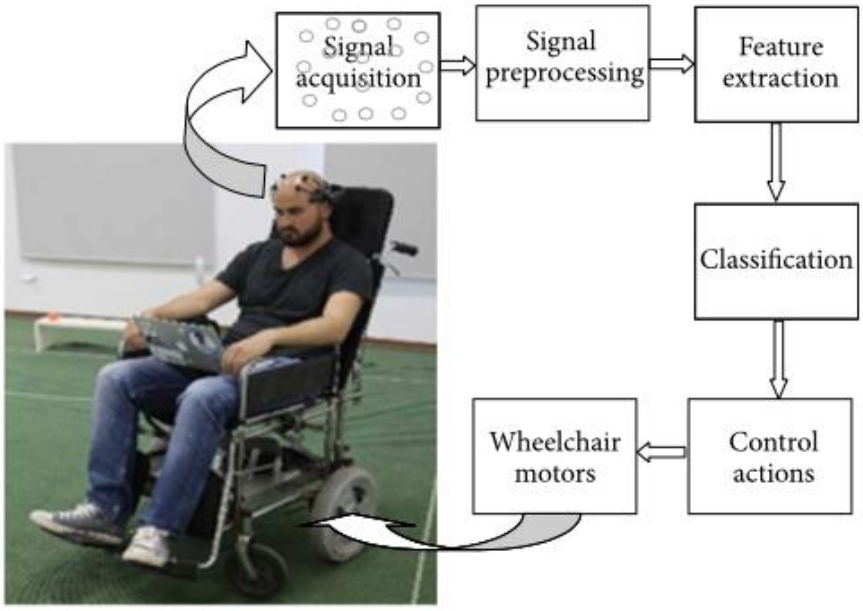

(Abiyev et al., 2016, [1]) [Figure 3.5.4: Control system flow for EEG controlled wheelchair using Fuzzy Neural Network]

Chapter 4: Technical Progress

4.1 Design

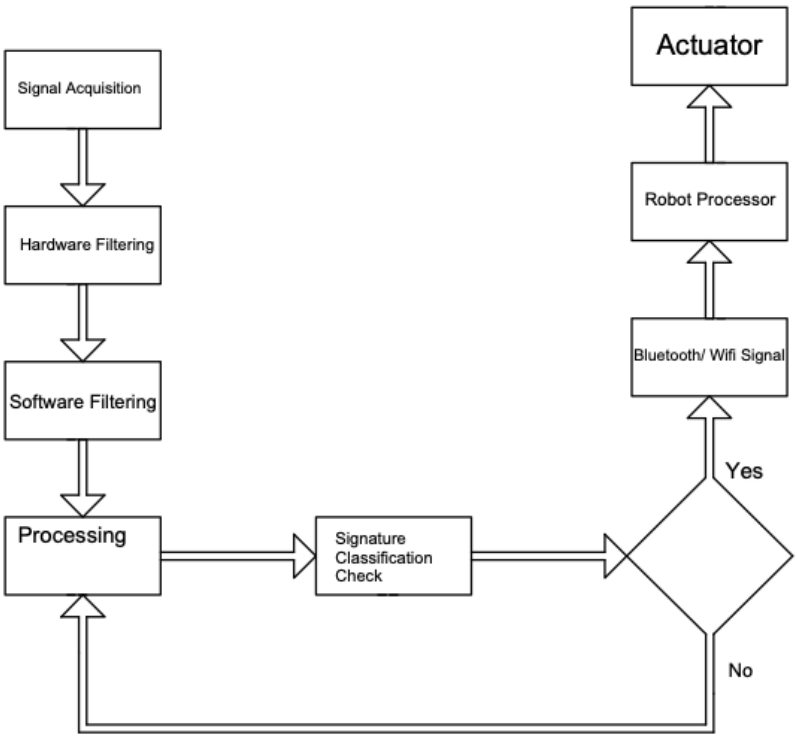

[Figure 4.1.1: State flow chart of signal acquisitions, filtering to switch signature verification resulting in some form of output (actuator) control]

Headset & Electrode Placement

In order to receive the signals, the headset was designed for secure, accurate placement of the electrodes at specific locations, allowing for small adjustments to be made when testing.

The electrodes that will drive the electronics were found from 'Unimed Electrode Supplies Limited'. The electrodes themself are 10mm in dimeter, 15cm in length and can be seen in figure 4.1.2. The electrodes have touch proof connectors conforming to DIN 42 802.

[Figure 4.1.2: Unimed Electrode Supplies Limited EEG electrodes with flat 10mm connection and conical centre & Electro-Gel conducting paste]

For a better connection to the scalp the electrodes are designed to be used with a conducting paste. This paste was also purchased from Unimed Electrode Supplies Limited.

The hat being used to connect the electrodes to secure positions has been repurposed from a cloth bicycle helmet inner. This can be seen in Figure 4.1.3.

[Figure 4.1.3: TAGVO thermal skull cap for securing electrode placement onto the scalp]

A chin strap was added to the skull cap in order to maintain the electrode positioning which is shown in the 'built' section, 4.2.

Following the placement in the 10-20 system shown in figure 3.2.1 and the Homunculus Map in figure 33.2. The electrodes will be roughly placed at positions C4 and C3 in order to receive signals coming from the motor cortex regions response to movement in the left and right arm. The placement will alter from person to person slightly depending on where the ridges in the skull are located.

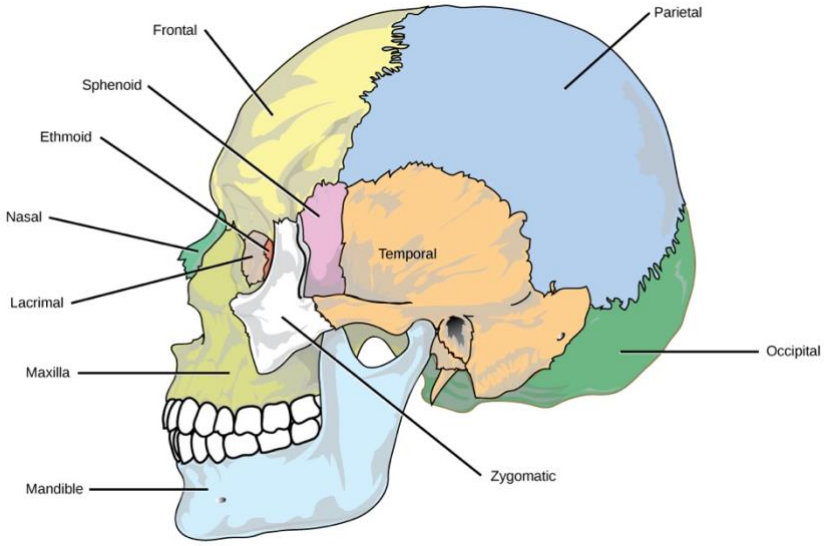

(Lumen [33]) [Figure 4.1.4: Structure of cranial and facial bones with the skull with corresponding names]

Using the ridge created at the boundary between the Frontal and Parietal lobes, electrodes were placed using this region to find the 'arm' associated motor area (see figure 3.3.2). For this research paper the area will be specific to the right and left arm but may not be the exact locations for the right/left bicep and triceps due to the relatively large region consisting of finger to shoulder activation seen in figure 3.3.2. Any signals from the correct arm will suffice for control.

The EEG will use three electrodes in total, one will be connecting to a reference point away from the brain, this will help remove some of the noise from resting potential on the skin. This reference electrode will pass through the instrumental amplifier into '-IN' meaning the difference between this signal and that of the active motor electrode will be taken and amplified

The second and third electrodes will be placed using the ridge line between the parietal and frontal boundaries along with the placement of C4 & C3 to best situate them for control over the arms. They will then be fed into the multiplexer which will cycle through the two electrodes allowing for them both to operate

The signals being picked up by the electronics are between $10\mu V \leq x \leq 30\mu V$, the signal is fed into the electronics for amplification and noise reduction. (cah6, 2012, [8])

Electronics

Given that the voltage read from the scalp will be in the range $10\mu V \leq x \leq 30\mu V$ the electronics will need to amplify this in stages up to a voltage ideally in the range $1mV < x < 1V$. This will be done in various stages with the ability to adjust the voltage gain within the hardware if needed.

Frequency filters will be needed to removed noise outside the data range. The first is a 50Hz notch filter to remove noise within UK systems, for use in America or other countries with different standard frequencies for their electronics this could mean altering some capacitor and resistor values within these 'notch' filters. The second filter will need to remove all noise above approximately 25Hz-30Hz as it will not be the useful data used for control. The third and final is a filter removing noise below approximately 7Hz. This data will not be of any use and could alter the results. Finally, the system will need to be able to take the difference between the galvanic skin response [natural potential of the skin] and the desired signals. This would be achieved using an instrumental amplifier with a reference node on a part of the head not possible for control use.

The system that was implemented was loosely based on one found from an Instructables post by 'cah6' though several elements have been changed which are discussed later. The schematic for the original electronics is found on Figure 4.1.5. The systems from 'cah6' only used one electrode but for control more will be needed where a multiplexer will be used to transfer from one electrode to another at set time intervals. The multiplexer output will be determined by an Elegoo microcontroller which follows the same design specifications as an Ardunio.

In order to test the functionality of each components before the build, bode plots were created using LTSpice software package or the frequency response calculator available at Okawa. The plots show how the gain of the signal is affected over a range of frequencies.

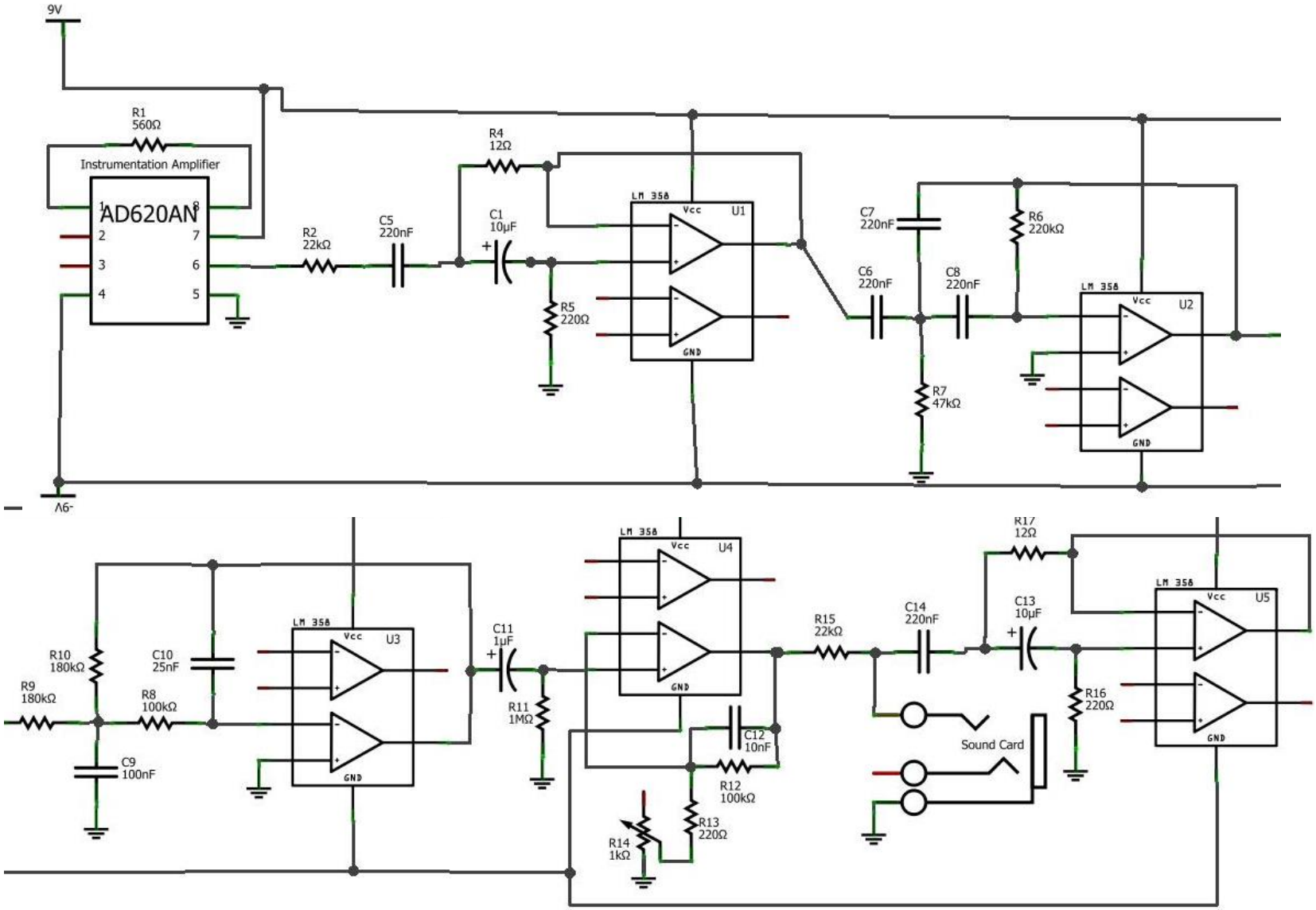

(cah6, 2012, [8]) [Figure 4.1.5: Template Electroencephalogram electronics circuit layout with one electrode from Instructables]

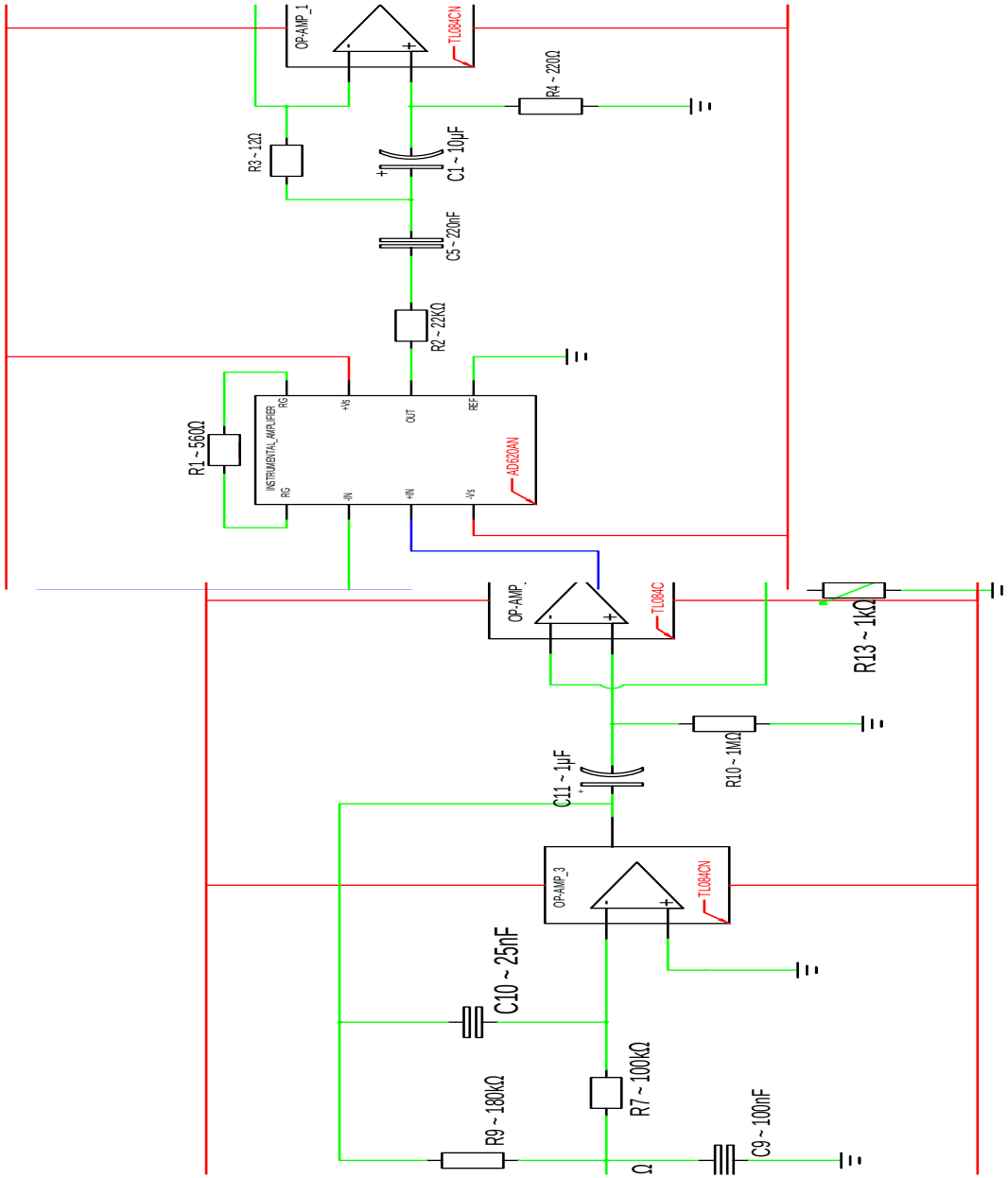

[Figure 4.1.6: Schematic iteration 1, 8:1 Electrode Electroencephalogram, with Arduino post processing (Key Pink: Ardunio, Green: Inner-wiring, Red: Power lines, Blue: Electrodes)]

Circuit Elements

A Multiplexer was integrated so that up to 8 electrodes could be incorporated in different locations on the scalp with one chosen to output into the instrumental amplifier at any instant.

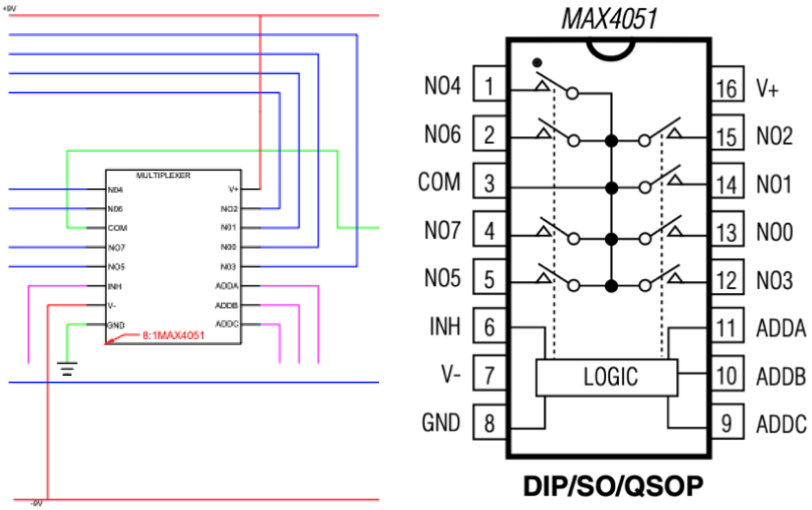

(MAXIM, 2005, [17]) [Figure 4.1.7: 8:1MAX4051 Low-Voltage Multiplexer]

The code describing how the multiplexer cycles through both the electrodes being used can be found in appendix A, figure A1. The signal is then sent into an instrumental amplifier according to the following gain equations.

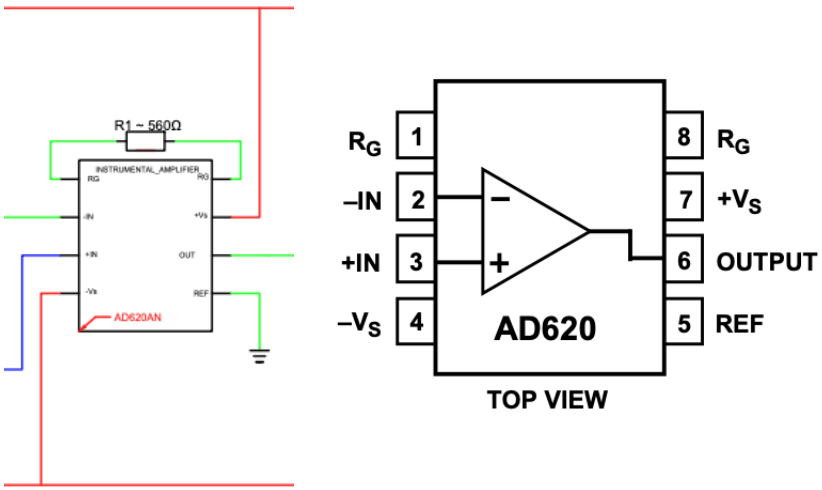

(Analog Devices, 2003 -2011, [2]) [Figure 4.1.8: Pin layout for AD620 chip with RG (Pin 1-8) set at 560Ω resulting in a gain of 89.2]

Taking the signal from the MUX and the reference signal from a nominal part of the scale the instrumental amplifier will take the difference between the two signals. The difference will then be amplified by a factor corresponding to the gain. This is set using a resistor between R_G (Pins 1 and 8).

$$Resistor\ Gain = \frac{49.4k\Omega}{G-1}$$

$$G = \frac{49.4k\Omega}{Resistor\ Gain} + 1$$

$$G = \frac{49.4k\Omega}{560\Omega} + 1 = 89.2$$

The final output follows the equation,

$$Vout = [(+IN) - (-IN)] * G \quad Volts$$

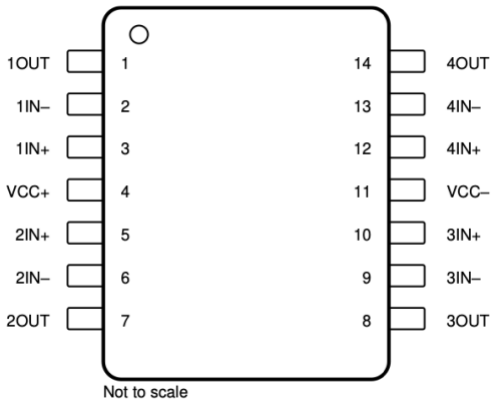

(Texas Instruments, 2020, [26]) [Figure 4.1.9: Pin layout for TL084CN Op-Amp Chip]

Several elements of the filtering and amplifying process will need an op-amp to function. This chip provides 4 on each. Two TL084CN chips where used for the five circuit elements.

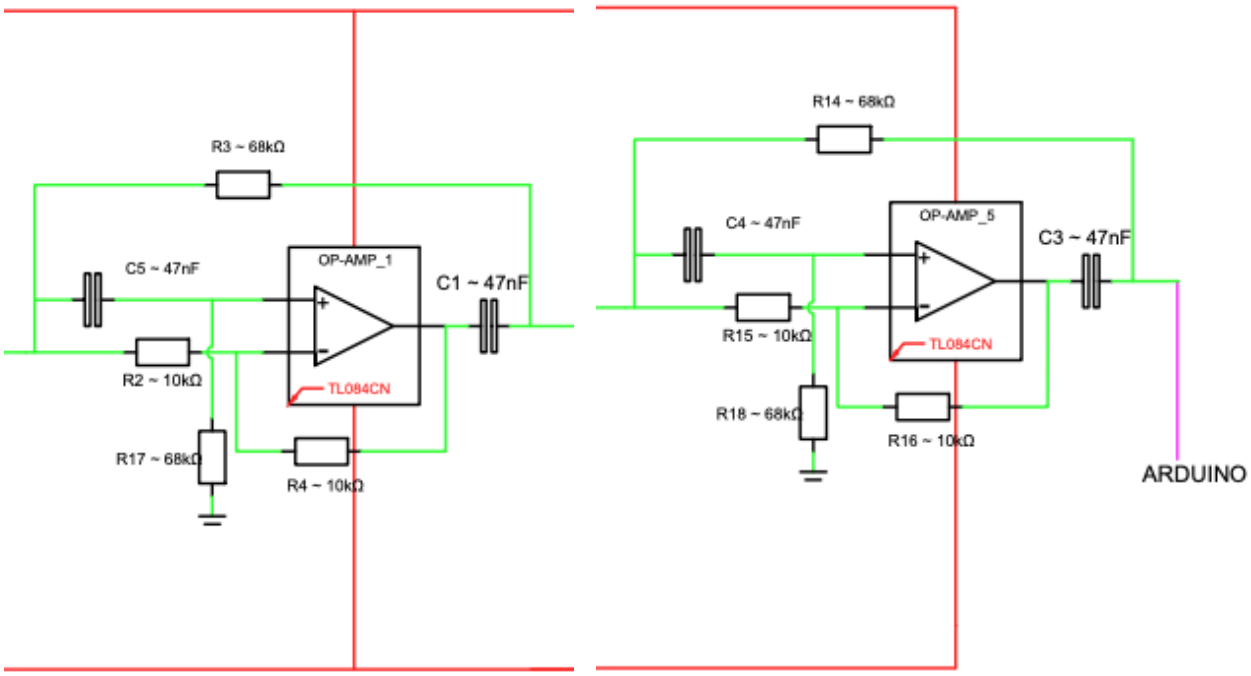

[Figure 4.1.10: Two 50hz active notch filters to remove general ambient noise in UK electronic systems]

The circuit uses two active notch filters to remove ambient noise around 50hz, which is specific for UK/European systems which operate at 50hz. The noise will still be present even if batteries are used to control the circuit. In order to remove the noise as effectively as possible, one filter is used at the beginning of the filtering stage and the second is used right at the end before the signal goes into the output terminal. The data being processed is in the range 8Hz < f < 27Hz so nothing of interest should get clipped.

$$Notch\ f = \frac{1}{2\pi RC}$$

$$50\ [hz] = \frac{1}{2\pi RC}$$

A reasonable value for capacitor, C = 47nF, making R

$$R = R2 = R4 = \text{R15} = \text{R16} = 10\ [\text{k}\Omega]$$
$$C = C1 = C3 = C4 = C5 = 47\ [nF]$$
$$R' = R3 = R14 = \text{R17} = \text{R18} = 68\ [\text{k}\Omega]$$

In order to avoid trimming using parallel resistors R2, R4, R15 & R16 need to be kept within 0.05% of their parallel counterpart. The frequency diagram below shows the gain dropping exponentially around 50Hz correlating to the desired operation.

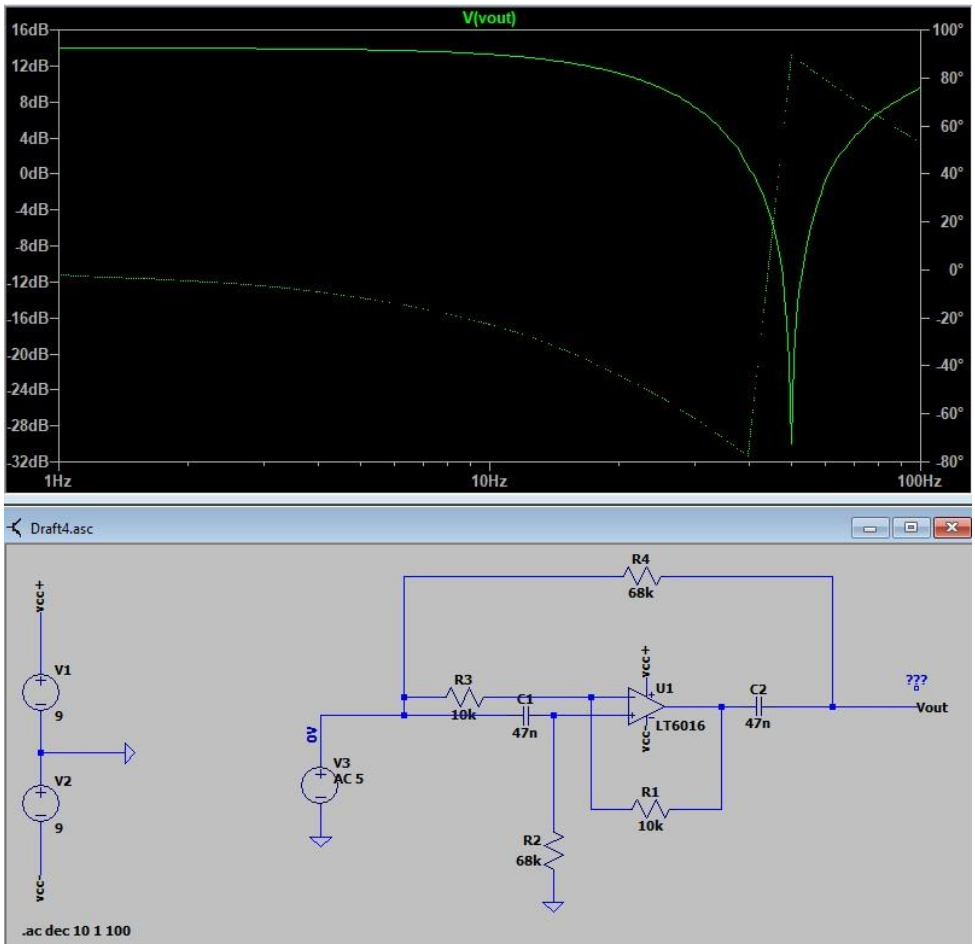

[Figure 4.1.11: AC frequency sweep analysis of the 50 Hz notch filter]

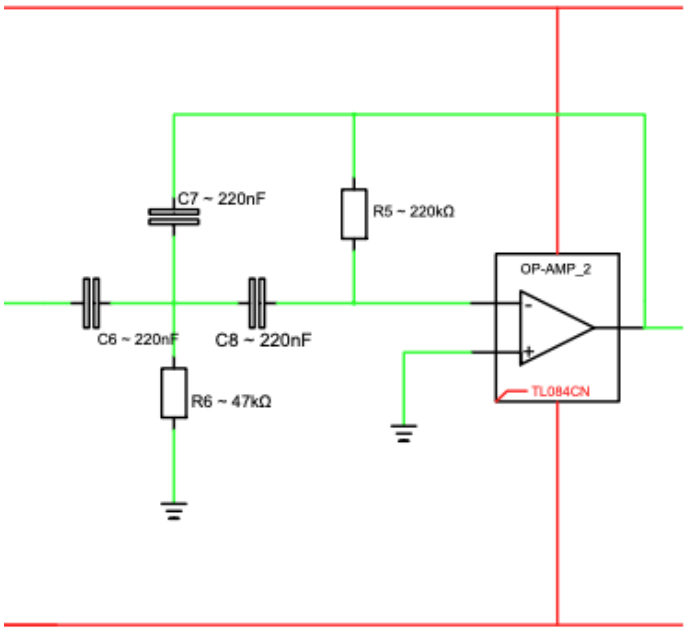

[Figure 4.1.12: 2 pole multi-feedback high-pass filter removing Electrodermal activity being picked up from the skin]

Electrodermal activity or the galvanic skin response causes continuous variation in the electrical properties of the skin. This means there is an element of this noise being picked up from the electrodes. The noise is of low frequency so a high pass filter centred around 7Hz should be sufficient to remove the noise.

The resistors and capacitors have been chosen to give the desired critical frequency, f_c and quality factor, Q which can be calculated by,

$$fc = \frac{1}{2\pi\sqrt{R5 * R6 * C8 * C7}}$$

$$fc = 7.11\ [Hz]$$

Where,

$$Q = 0.721$$

With a cut-off frequency f_c of 7.11Hz the gain will be at roughly 72% at this frequency. From this point the gain will decrease exponentially as the frequency approaches 0Hz. Above f_c the gain will quickly approach 1, meaning the frequencies past this will be unaffected shown in figure 4.1.13.

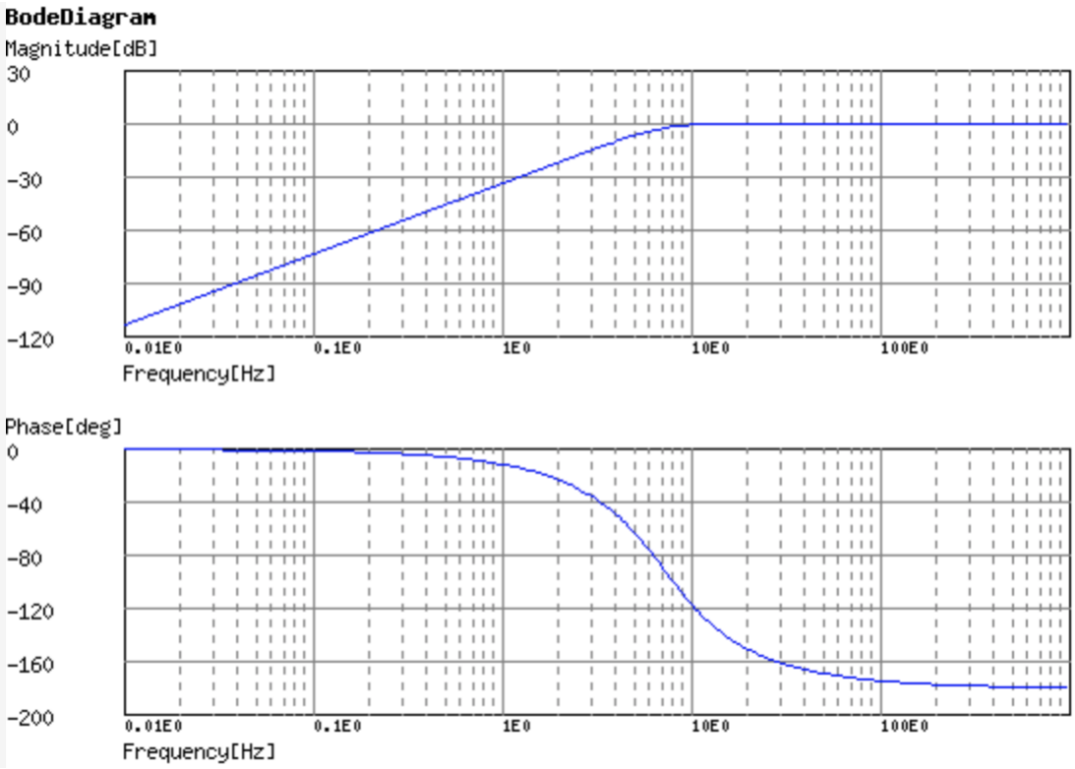

(OKAWA,2004, [19]) [Figure 4.1.13: Magnitude (dB) & Phase (Degrees) v Frequency (Hz) of the 2 pole multi-feedback high-pass filter centred at 7.11Hz]

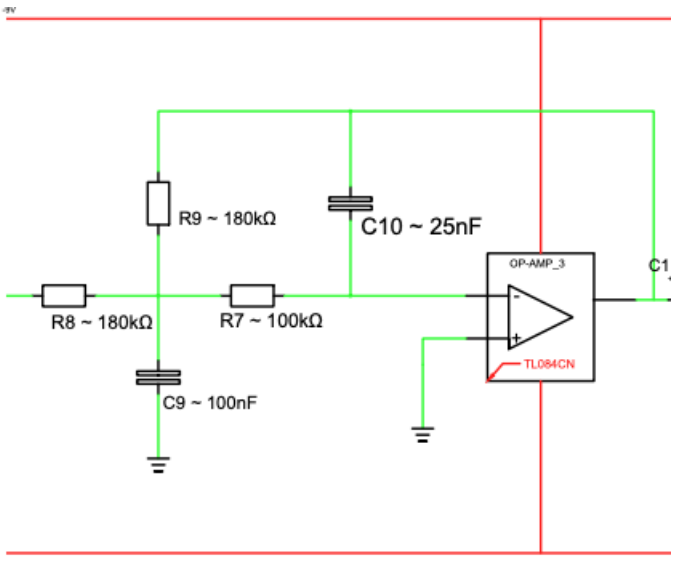

[Figure 4.1.14: 2-Pole multi-feedback low-pass filter centred at 23.73hz]

The purpose of this filter is to remove all the data with frequencies higher than 27Hz as much of this will be noise. It also will not affect the range of frequencies that are being inspected for control.

Although the filter is set for a 23.73Hz centre it operates with a gain of 0.71 at 31.23Hz. Above this value the gain drops off rapidly to a point at 300Hz the gain is 0.01. With the values given the critical frequency, f_c

$$fc = \frac{1}{2\pi\sqrt{R7 * R9 * C10 * C9}}$$

$$fc = 23.73\ [Hz]$$

Where the quality factor is,

$$Q = 0.706$$

The response can be seen in the following graphs

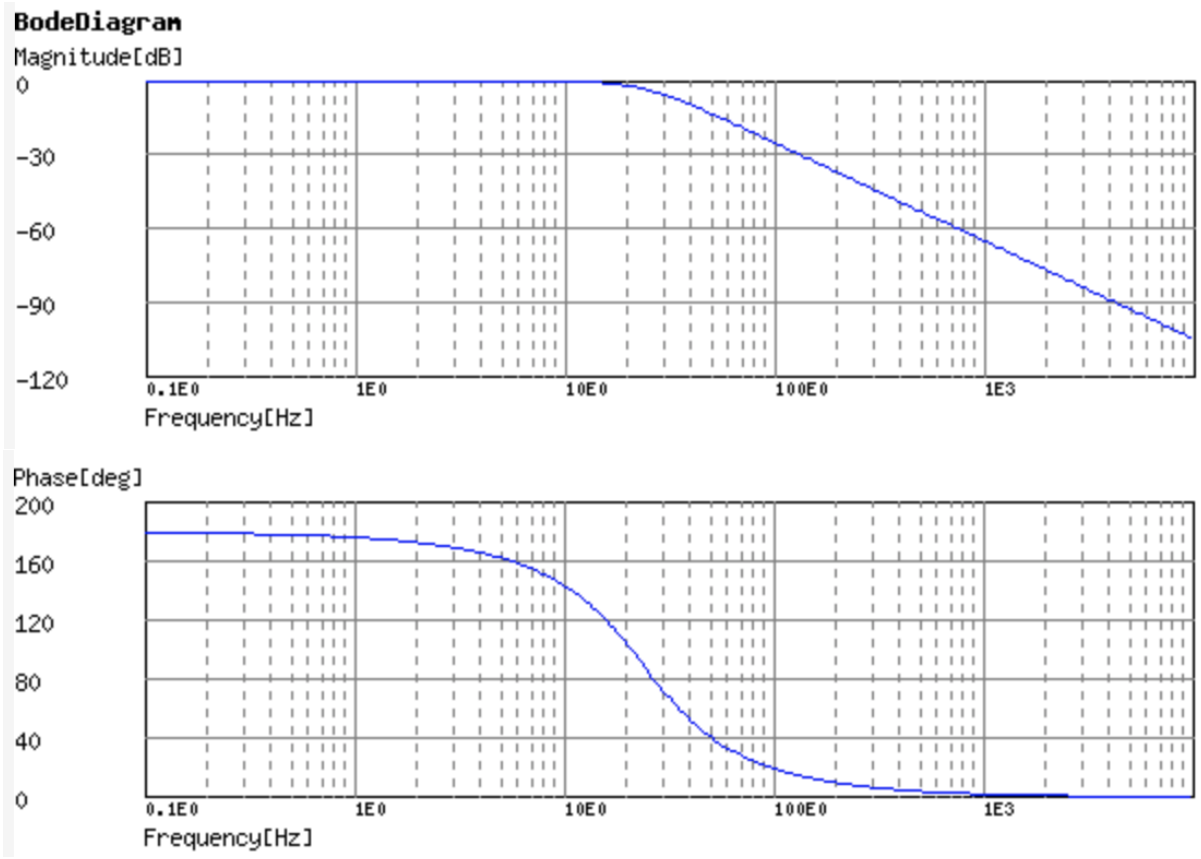

(OKAWA,2004, [19]) [Figure 4.1.15: Magnitude (dB) & Phase (Degrees) v Frequency (Hz) of the 2-Pole multi-feedback low-pass filter centred at 23.73]

An issue arose when trying to buy a 25nF capacitor. The only ones available were for high voltage protection which this circuit does not need. For this reason, the values of the capacitors and resistors were changed so that the outcome would be the same but with accessible components.

Using the calculators made available at 'OKAWA Electric Design' the values of the components have been changed such that,

$$C10 = 0.33\mu F, \qquad C9 = 3.3\mu F, \qquad R7 = 12k\Omega, \qquad R8 = 3k\Omega, \qquad R9 = 3k\Omega$$

$$\frac{1}{2\pi\sqrt{R7 * R9 * C10 * C9}}$$

$$fc = 25.42\ [Hz]$$

And the quality factor (Q) determined,

$$Q = 0.706$$

The cut-off frequency has been changed to a slightly higher frequency to avoid cutting off data in the range $7 \leq f \leq 30$ [Hz] by as much as possible. At 32Hz the gain will be roughly 0.71, decreasing dramatically from this point. The frequency graphs follow,

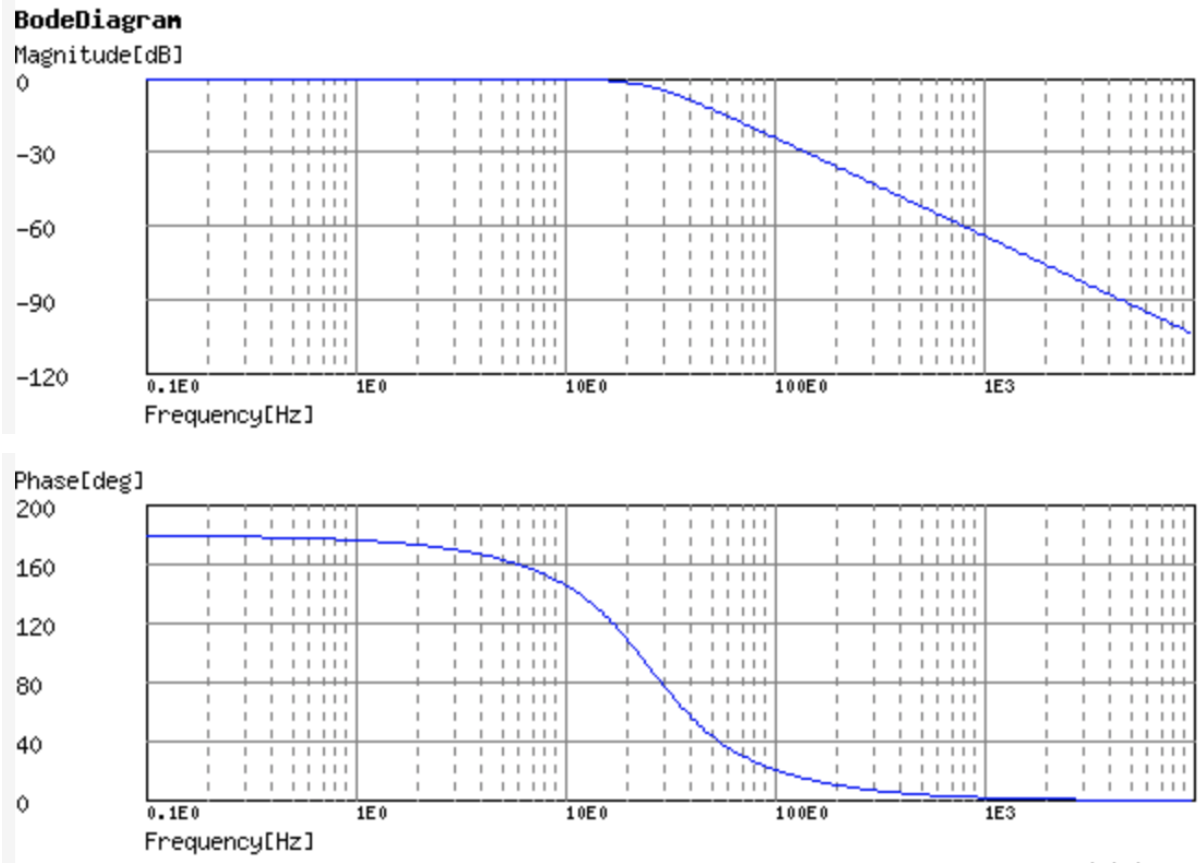

(OKAWA,2004, [19]) [Figure 4.1.16: Magnitude (dB) & Phase (Degrees) v Frequency (Hz) of the 2-Pole multi-feedback low pass filter centred at 25.42]

The next module simulated was a non-inverting amplifier with low frequency high-pass filter. The high-pass filter removes very low frequencies while also making the non-inverting amplifier more responsive at lower frequencies below approximately 13 Hz.

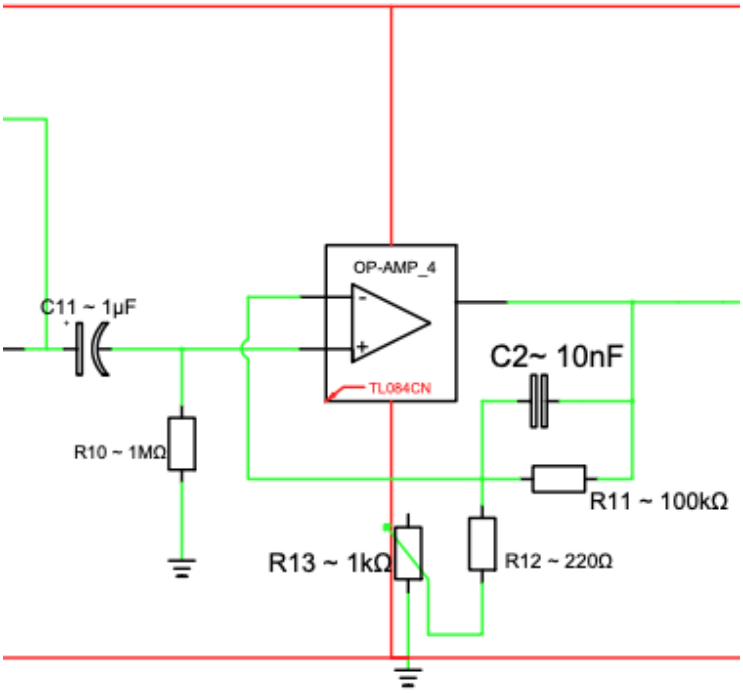

[Figure 4.1.17: Non-inverting amplifier with 1kΩ gain control]

$$fc = \frac{1}{2\pi * R10 * C11}$$

$$fc = 0.1591\ [Hz]$$

C2 and R11 perform a high-pass filter with a cut-off f_c of,

$$fc = \frac{1}{2\pi * R11 * C2}$$

$$fc = 159.15\ [Hz]$$

Both of these filters remove small amounts of unwanted noise. The main purpose of this non-inverting amplifier is to implement adjustable gain using the potentiometer placed at R13

$$\frac{Vout}{Vin} = G = 1 + \frac{R11}{R12 + R13}$$

Thus implying,

$$82.96 \geq G \geq 455.5$$

Using this and the gain attenuated in the instrumental amplifier the voltage after the electronics should be in the range,

$$0 \leq Vout < 1\ [Volts]$$

With the amplitude of the input single voltage from a given persons head ranging from,

$$10\mu \leq Vin \leq 30\mu\ [Volts]$$

The output voltage of the signal into the Elegoo will be, using a 20µV sample, in the range,

$$0.1481 \leq Vout \leq 0.8126\ [\text{Volts}]$$

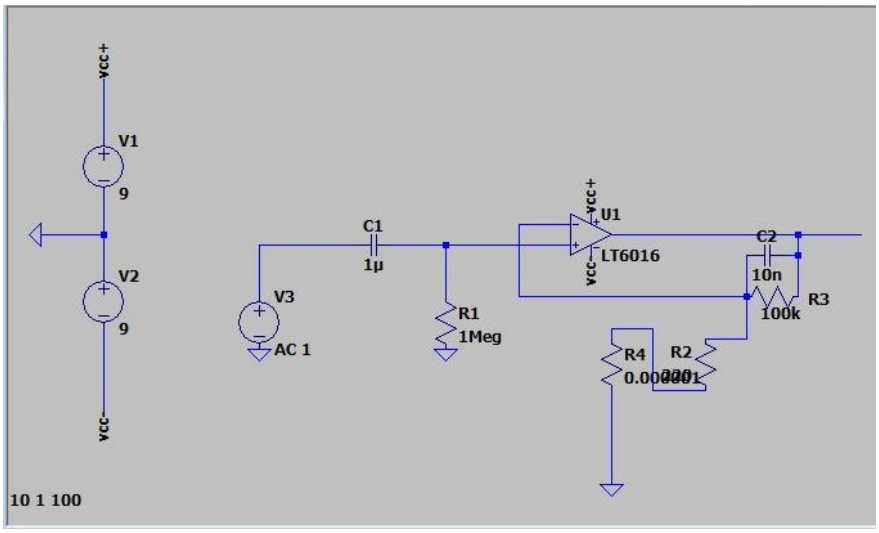

[Figure 4.1.18: simulations of non-inverting amplifier with adjustable gain]

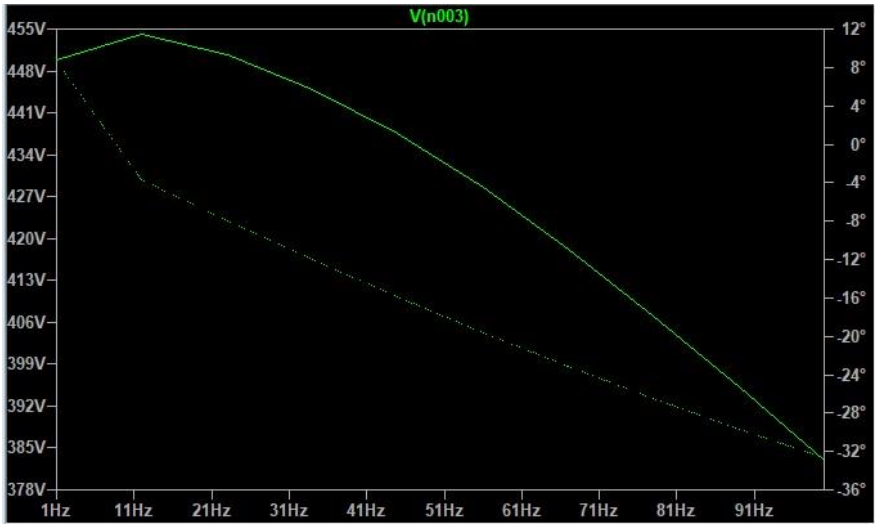

[Figure 4.1.19: AC sweep analysis of high-end adjustable gain non-inverting amplifier, R12 (R4 in simulation) set to approximately 0Ω]

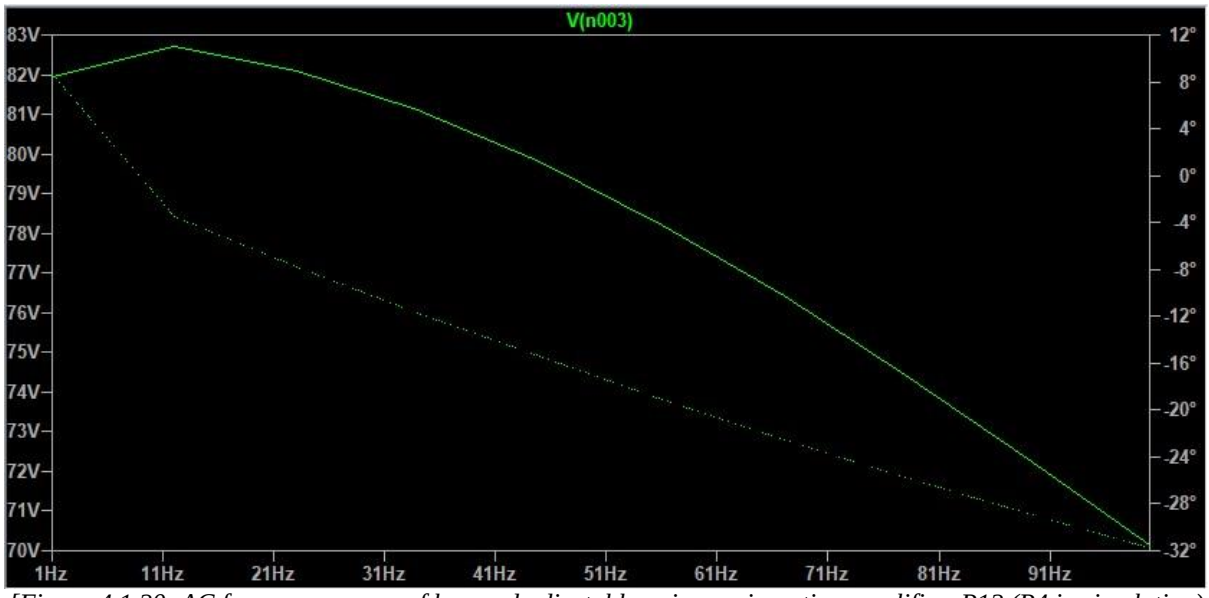

[Figure 4.1.20: AC frequency sweep of low-end adjustable gain non-inverting amplifier, R12 (R4 in simulation) set to 1kΩ]

Both of the AC frequency sweep graphs show the Vout response when passed through the non-inverting amplifier over a range of 100 Hz with a 1V input signal.

The full system was tested without the multiplexer or instrumental amplifier to see the gain and filtering through a frequency sweep.

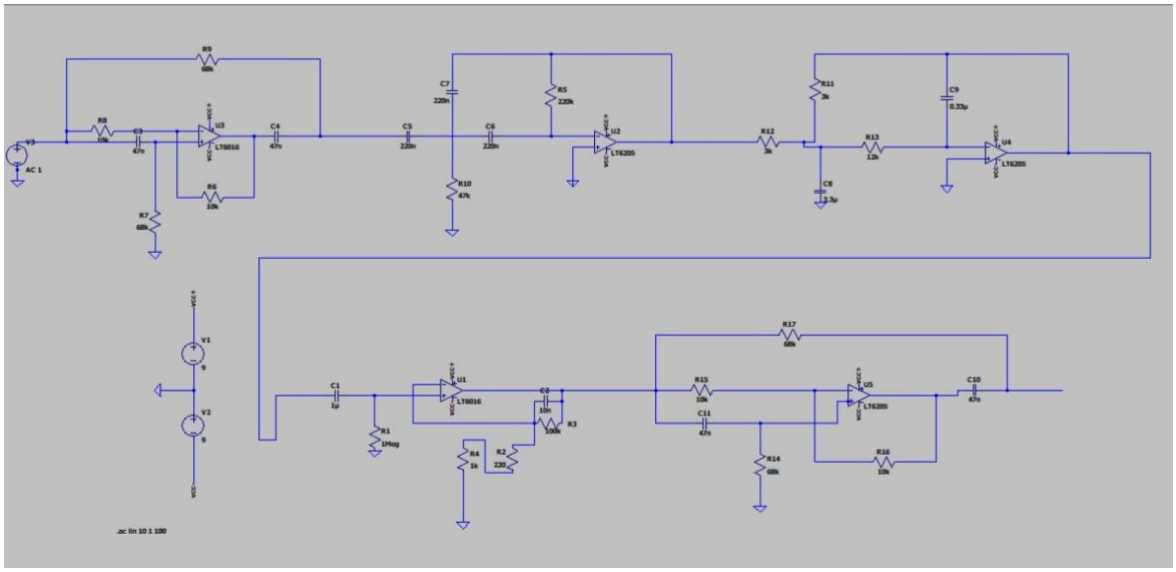

[Figure 4.1.21: Simulation schematic of 50Hz notch filter, 2-pole multi-feedback low-pass filter, 2-pole multi-feedback high-pass filter, non-inverting amplifier and output 50Hz notch filter]

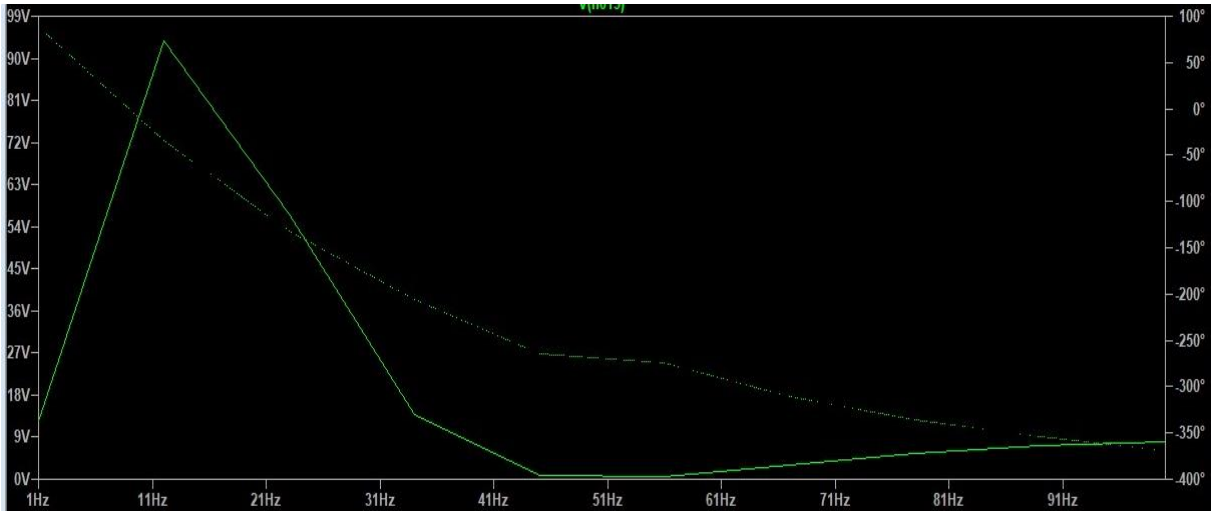

[Figure 4.1.22: AC sweep analysis of system filtering and gain response when R13 is get to 1kΩ, without gain from the instrumental amplifier]

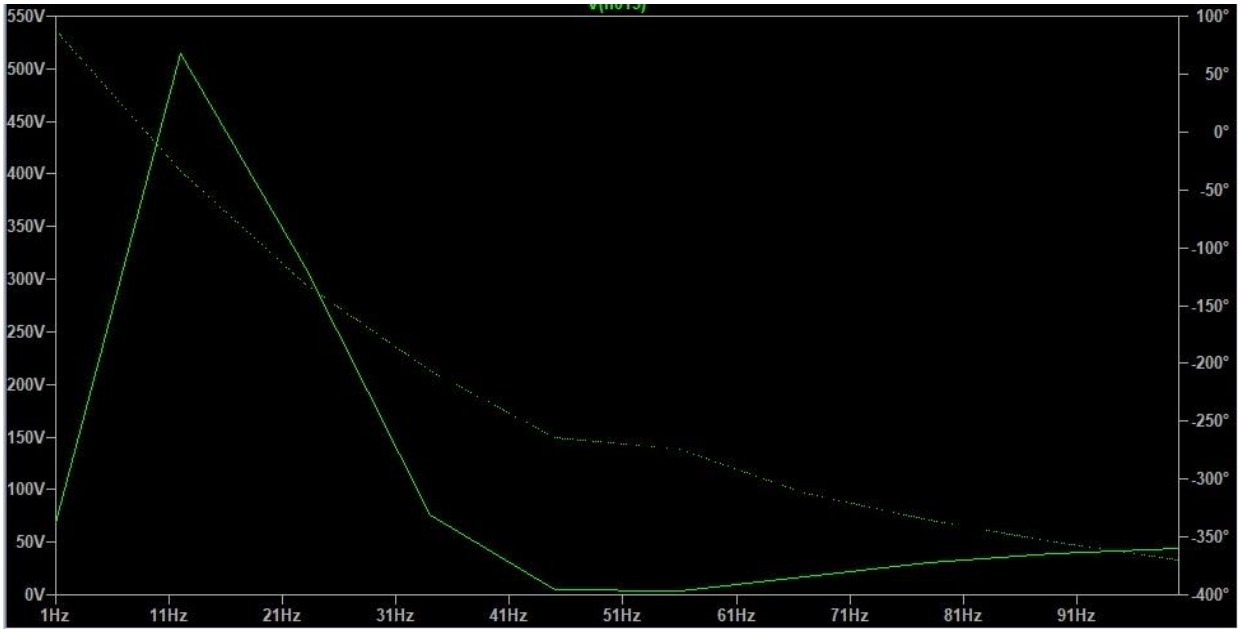

[Figure 4.1.23: AC sweep analysis system filtering and gain response when R13 is get to approximately 0Ω, without gain from the instrumental amplifier]

The response from the system tests show that the gain will peak at roughly 13hz which is on the lower centre of the data which is intended for control. The values for both systems will be offset by the additional gain of the instrumental amplifier calculated as above in figure 4.1.8 and testing below.

Using a test voltage of 20µV, taking an average of the gain across the 10-20hz range.

$$20\mu V * 72 < Vout < 20\mu V * 400\ (Volts)$$

$$0.000144 < Vout < \ 0.0008\ (Volts)$$

When adding the offset of the instrumental amplifier

$$0.1296 < Vout < 0.72\ (V)$$

The is within the planned range of Vout < 1V

In order to power the electronics and the Elegoo, two 9-volt batteries have been connected with one in reverse. This has been done in order to establish a +9V and -9V terminal to power the op-amps, instrumental amplifier and multiplexer chips.

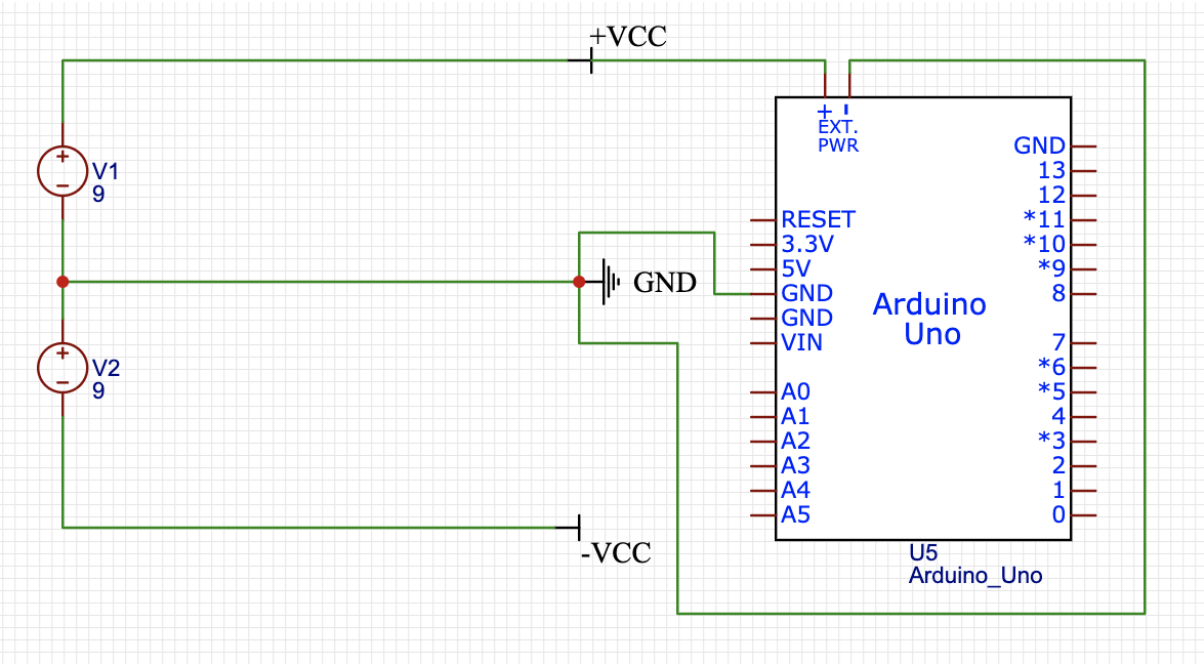

[Figure 4.1.24: Power supply system for connecting to Elegoo and EEG Electronics]

The final circuit used can be seen below in figure 4.1.25.

A full list of the components used for the build section can be seen in figure 6.3.1 and 6.3.2 withing the budget management chapter.

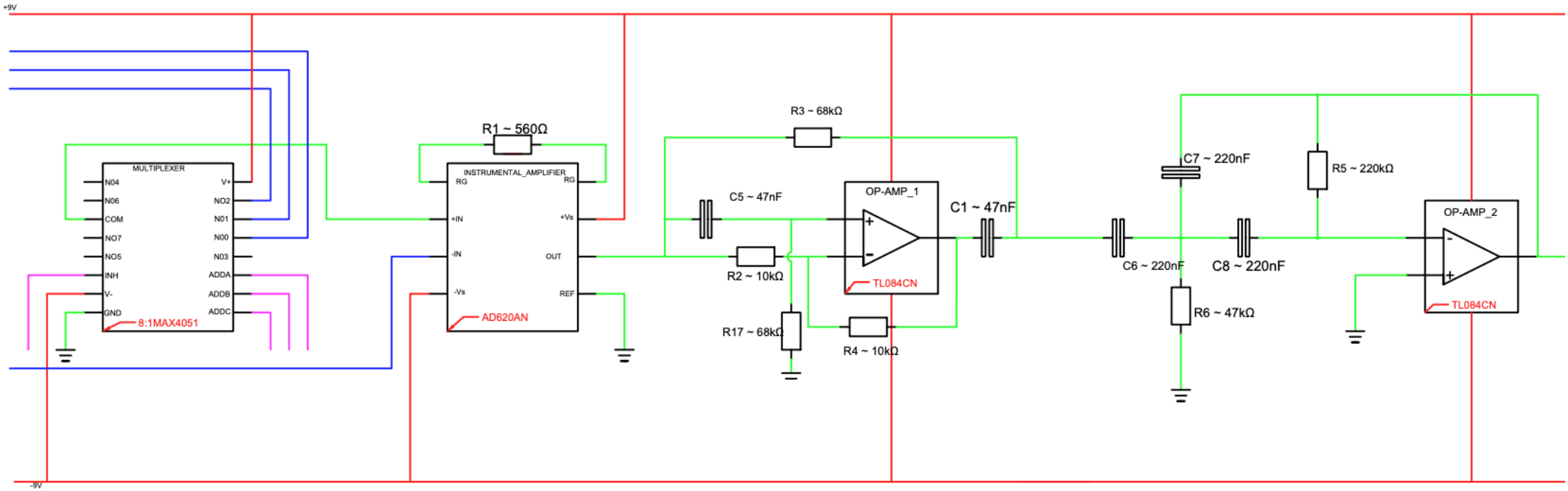
+9V
MULTIPLEXER
N04
N06
COM
NO7
NO5
INH
V-
GND
V+
NO2
N01
N00
N03
ADDA
ADDB
ADDC
8:1MAX4051
R1 ~ 560Ω
INSTRUMENTAL_AMPLIFIER
RG
+IN
-IN
-Vs
+Vs
OUT
REF
AD620AN
R3 ~ 68kΩ
C5 ~ 47nF
OP-AMP_1
C1 ~ 47nF
R2 ~ 10kΩ
TL084CN
R17 ~ 68kΩ
R4 ~ 10kΩ
C7 ~ 220nF
R5 ~ 220kΩ
OP-AMP_2
C6 ~ 220nF
C8 ~ 220nF
R6 ~ 47kΩ
TL084CN
-9V

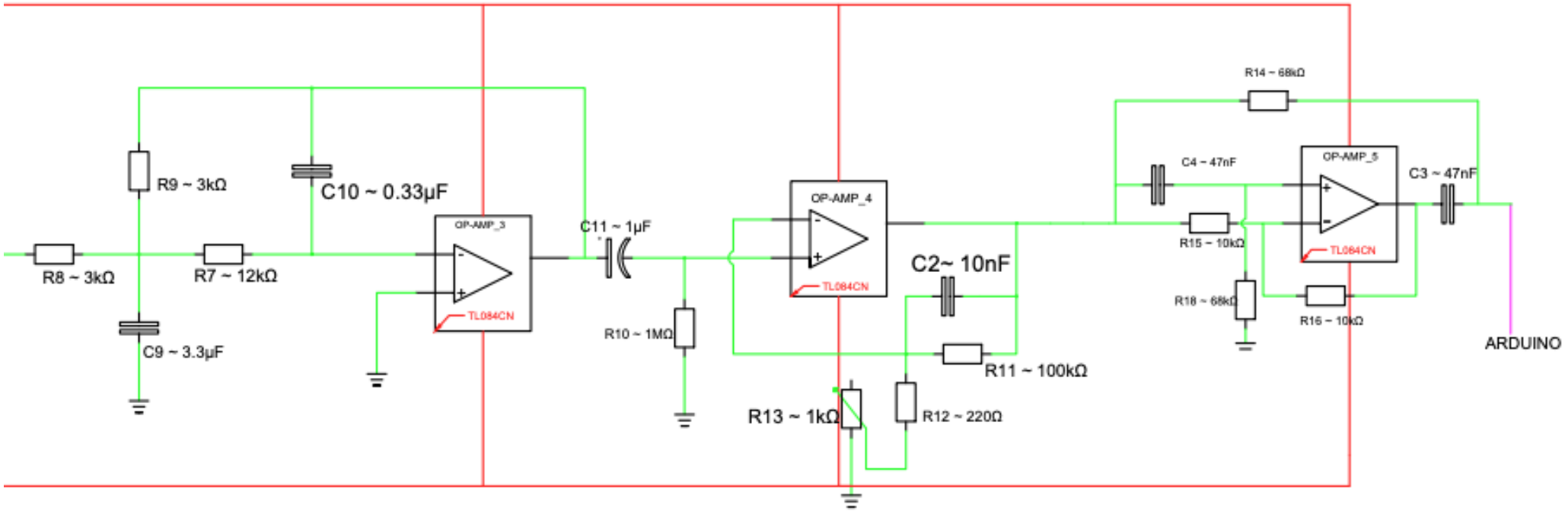

[Figure 4.1.25: Schematic iteration 2, Notch filter Op-Amps 1 & 5 now centred around 50Hz, Adjustable gain non-inverting amplifier components changed (Key Pink: Ardunio, Green: Inner-wiring, Red: Power lines, Blue: Electrode)]

4.2 Build

Headset Build

The first thing that was built on to the headset was a strap to help secure the position of the electrodes.

[Figure 4.2.1: Strap sewed onto headset to maintain electrode positions while testing]

The ridge line connecting the parietal and frontal cranial bones was located by touch and a white line was drawn with reference taken from the cortical bones (figures 4.1.4), the homunculus map (figure 3.3.2) and the cortical regions (figure 3.3.1).

[Figure 4.2.2: White lines on cranial ridge between partial and frontal regions of the skull]

Looking more specifically at the homunculus map from figure 3.3.2 the regions of activity for the arms were located and electrodes were sewn into place. They have been sewn in slightly behind the cranial ridge so that small adjustments can be made for a better fit.

[Figure 4.2.3: Electrodes situated on the scalp in positions corresponding to the cortical motor regions of the arms]

Two electrodes were placed to read activity in the regions of the motor cortex associated with the arms. The third, reference electrode was placed on the lower left side of the frontal cranial bone above the zygomatic bone (see figure 4.1.4). This region was chosen due to the thickness of the skull, making it much less susceptible to conductive activity from the brain.

As seen in figure 4.2.3 and the connected board (figure 4.2.25) The white ‘reference’ electrode was connected to the instrumental amplifier as -Vin and green and yellow ‘active’ electrodes were connected to N00 and N01 as inputs to the multiplexer. The electrode sent through the encephalogram will be determined by the logic selection within the Elegoo code (figure A1 & A2).

Breadboard Build

The system was broken down to the individual modules of the circuit to test correct functionality. Due to the circuit requiring such low voltages a full system test was not possible on a breadboard as the waveform generator could not output such small voltages without it being totally distorted due to effects like the probe wires acting as antenna, picking up small signals from local devices.

When testing using voltages on a millivolt scale waveforms where adjusted to remove this noise by averaging over 16-128 waveforms.

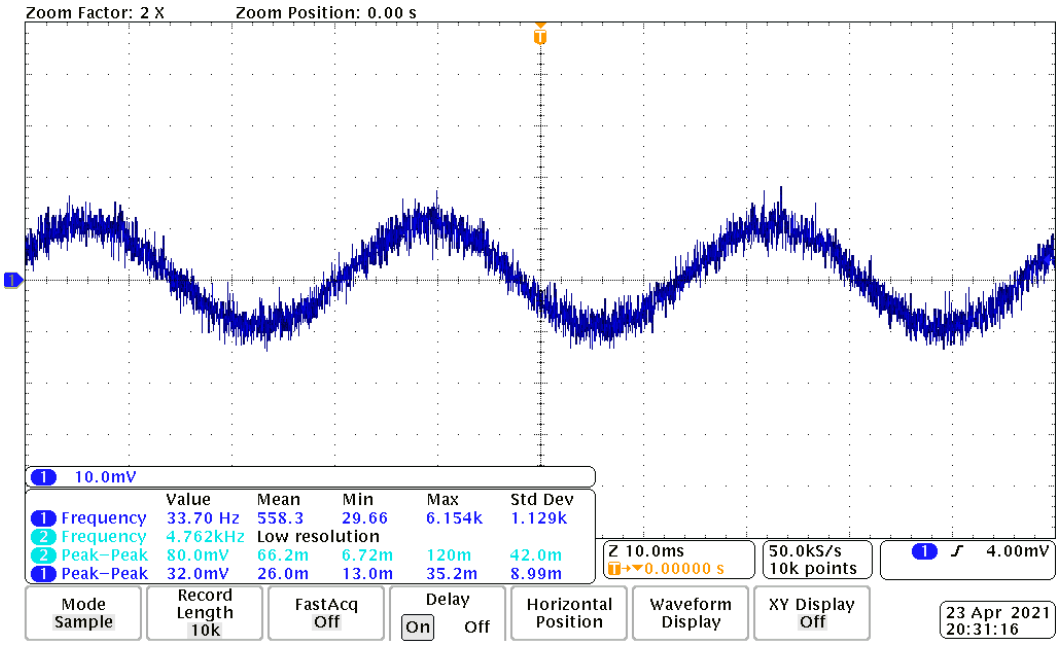

[Figure 4.2.4: 30Hz, 20.0mV peak-to-peak signal sample without averaging]

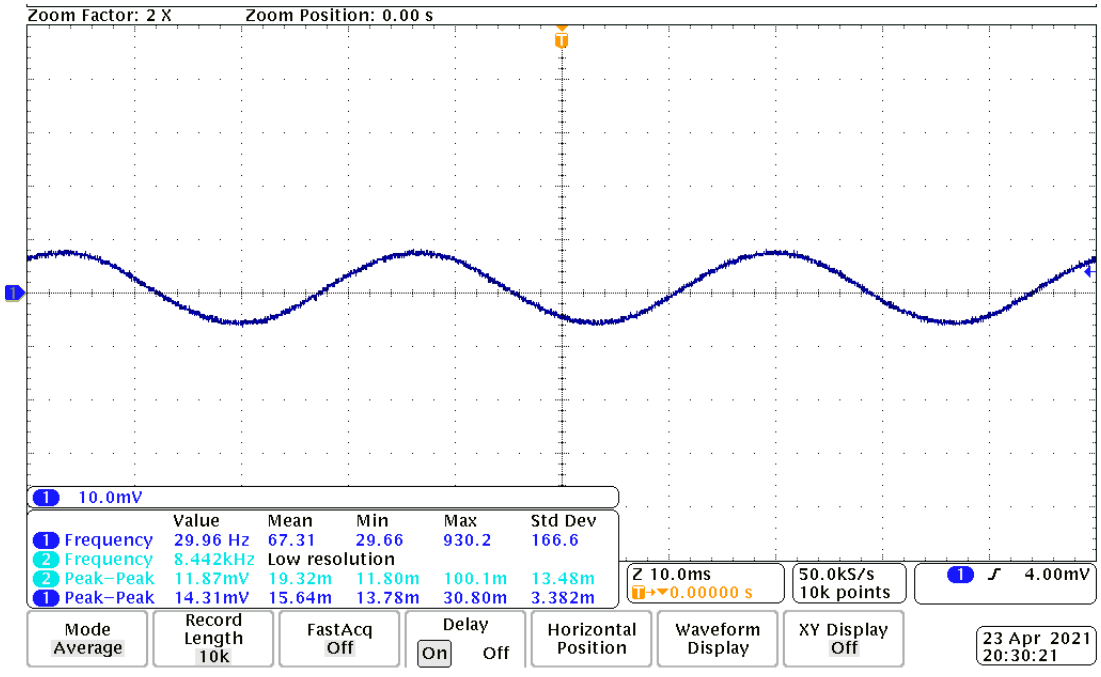

[Figure 4.2.5: 30Hz, 20.0mV peak-to-peak signal averaging enabled to remove antenna noise from probes]

It might be possible to get around this by implementing a faraday cage with the breadboard circuit inside though it is unclear if this would be enough to test using µV scale.

The first module tested was the instrumental amplifier to check the gain from a low-voltage input range. It was constructed as shown in figure 4.2.6 with figure 4.1.8 showing pin connections.

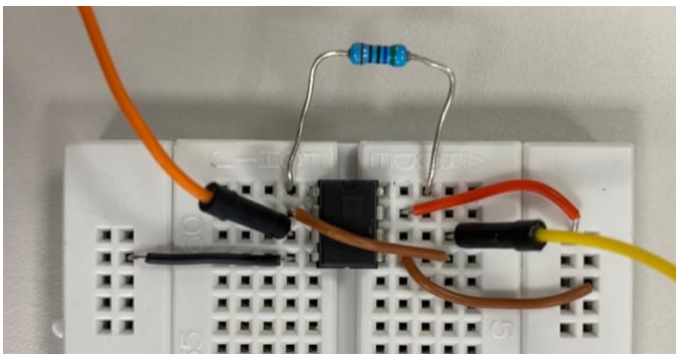

[Figure 4.2.6: Connections of Instrumental Amplifier to check gain (Red: +9V, Black: -9V, Brown: Ground, Yellow: Vout, Orange: Vin)]

Sent into Vin was a fixed 20Hz signal with amplitude voltage ranging from $0.01 < V < 0.1$ (volts).

From the data collected the gain was found,

$$G = 93.9$$

The data can be found in appendix B

The 50Hz notch filter was tested in conjunction with the instrumental amplifier. The input voltage was fixed at 0.03V with a range of frequencies being explored.

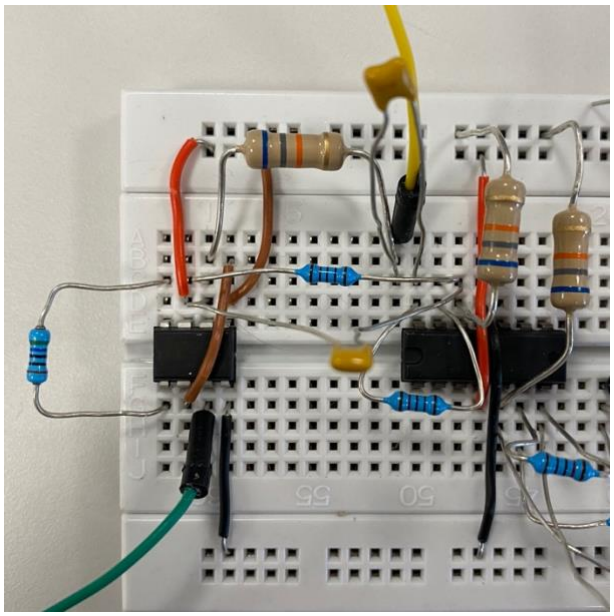

[Figure 4.2.7: *Connections of Instrumental Amplifier and 50Hz notch filter (Red: +9V, Black: -9V, Brown: Ground, Yellow: Vout, Green: Vin)]*

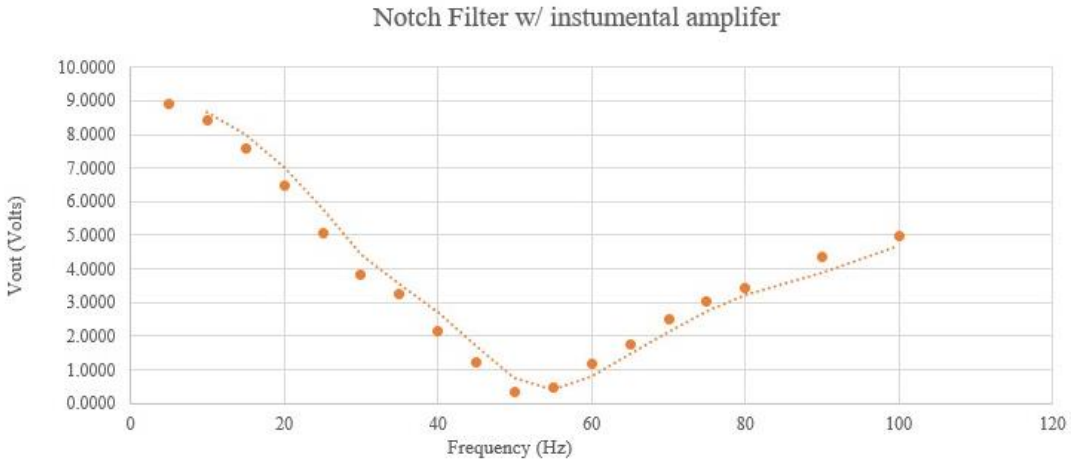

[Figure 4.2.8: Vout vs frequency response 50Hz notch filter with input through instrumental amplifier]

The scaling is different to that of the simulations, hence the different graphs. Data for this can be found in appendix B.

The next module tested was the 2-pole multi-feedback high-pass filter centred at 7.11 Hz

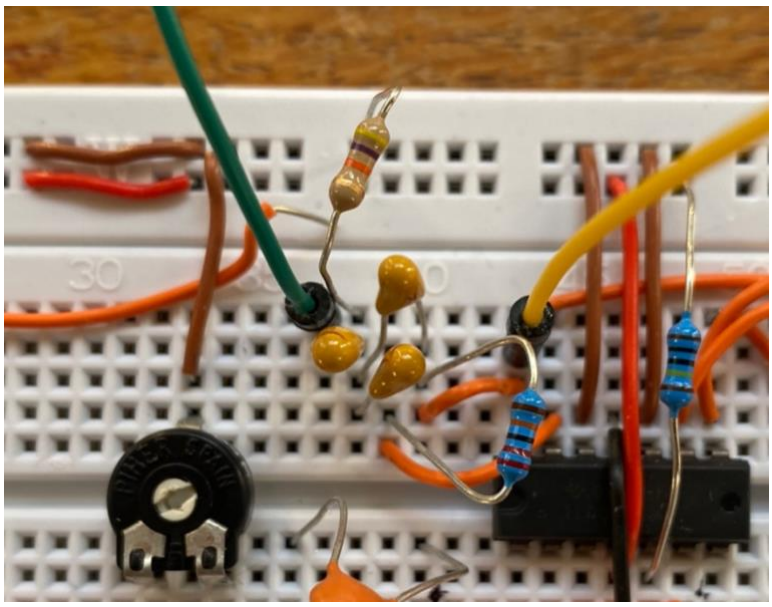

[Figure 4.2.9: *Connections of 2-pole multi-feedback high-pass filter (Red: +9V, Black: -9V, Brown: Ground, Yellow: Vout, Green: Vin)]*

Again, this was tested with a range of frequencies with a constant voltage of 250mV applied at Vin

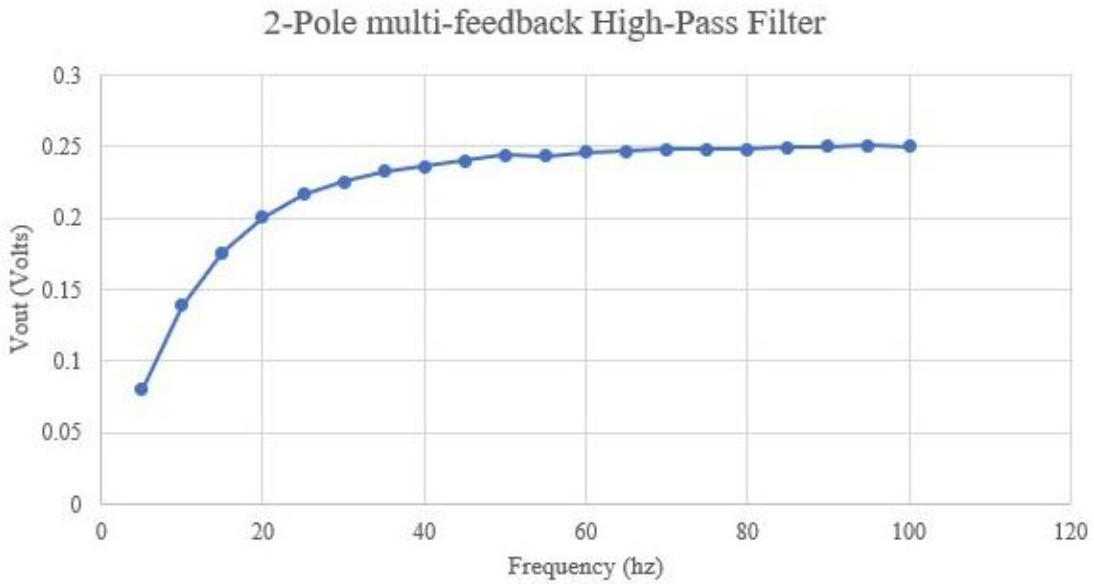

[Figure 4.2.10: Vout vs frequency response of 2-pole multi-feedback high pass filter centred at 7.11 Hz]

Data for this testing can be found in appendix B.

The next module tested was the 2-pole multi-feedback low-pass filter centred at 23.73 Hz shown on the breadboard below.

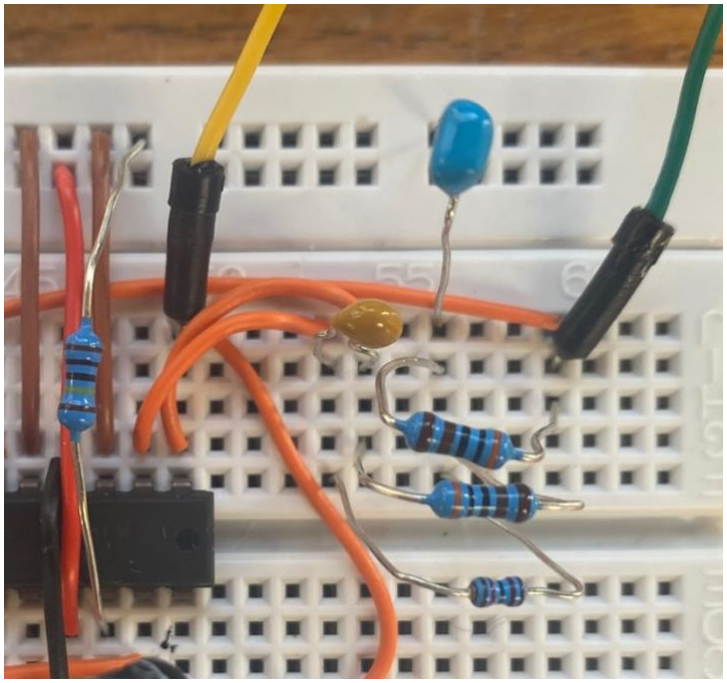

[Figure 4.2.11: Connections of 2-pole multi-feedback low-pass filter (Red: +9V, Black: -9V, Brown: Ground, Yellow: Vout, Green: Vin)]

This module was tested in the same way as the high-pass filter with an AC sweep from 1 - 100 Hz.

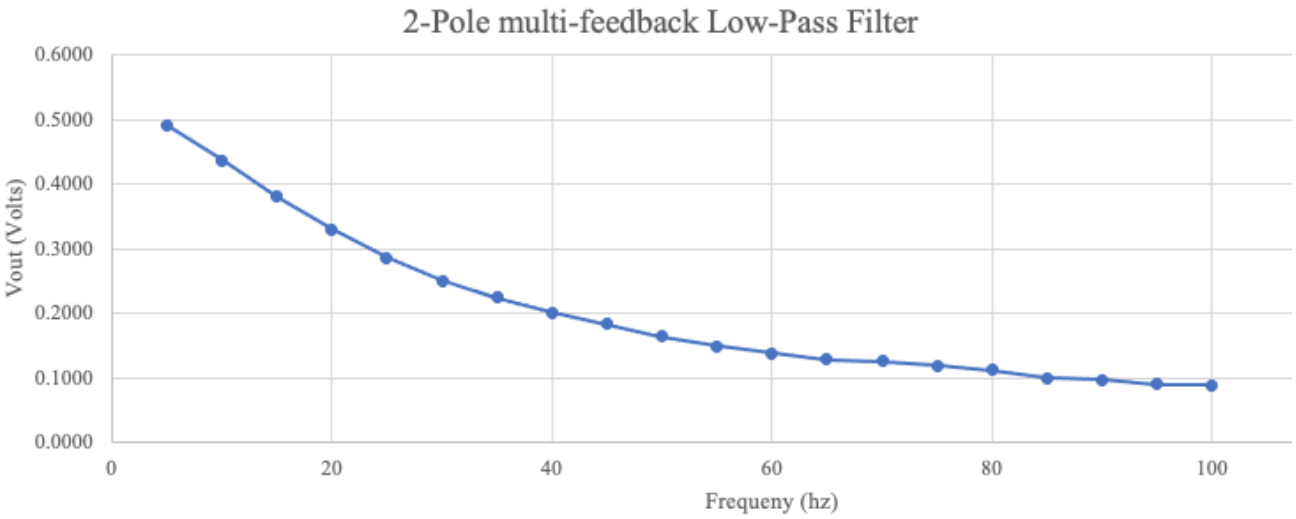

[Figure 4.2.12: Vout v Frequency response of 2-pole multi-feedback low-pass filter]

The non-inverting amplifier was tested twice, once with R13 set to approximately 0Ω with an expected gain of 455.5 and then with R13 set 1kΩ with a gain of 82.9.

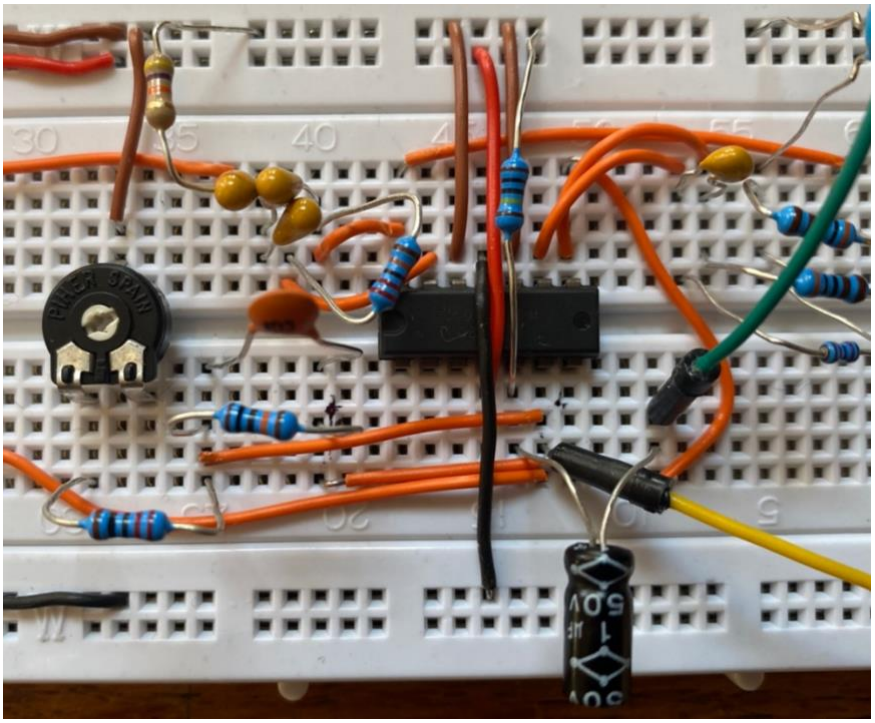

[Figure 4.2.13: Connections of non-inverting amplifier with adjustable gain using R13 (Red: +9V, Black: -9V, Brown: Ground, Yellow: Vout, Green: Vin)]

The data values from the non-inverting amplifier can be seen in figure B. The gain averaged from the data has a range of,

$$75.9 < G < 399.2$$

Though these values are low, the voltage range for the output is still within the desired mV scale. The inaccuracy is mainly due to excessive use of the variable resistor which does not have the most reliable rotary system for adjusting gain. To ensure maximum performance when using the PCB, a new resistor was acquired for R13 form the labs.

With the gain shown from testing of the instrumental amplifier, the total system gain is in the range,

$$7127 < G < 37484.9$$

With a 20µV input, Vout will be in the range

$$0.1425 < Vout < 0.7497\ Volts$$

The last module tested was the 50Hz notch filter

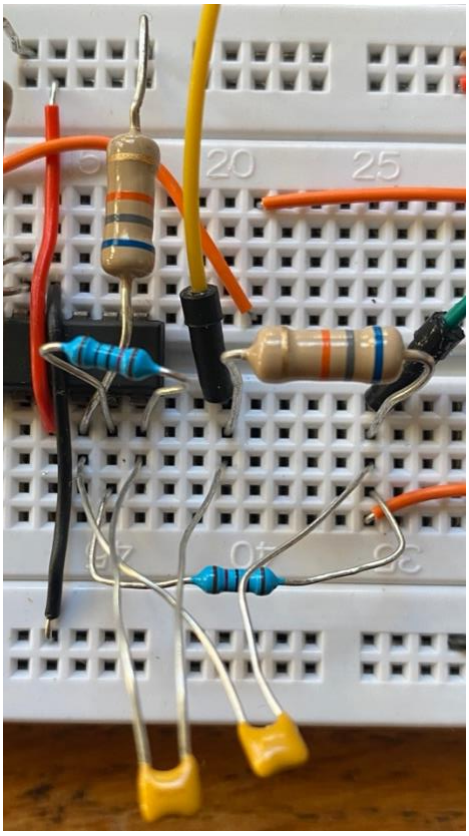

[Figure 4.2.14: Connections 50hz notch filter R13 (Red: +9V, Black: -9V, Brown: Ground, Yellow: Vout, Green: Vin)]

The output data can be seen in figure 4.2.15 with the testing data in figure B6 within appendix B

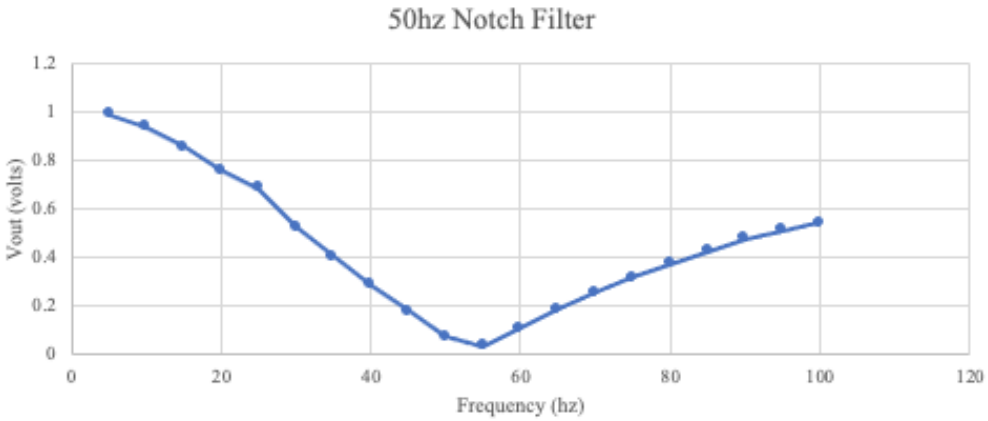

[Figure 4.2.15: Vout v Frequency testing of 2-pole multi-feedback low-pass filter]

This completed the breadboard testing with the full system shown on a breadboard below

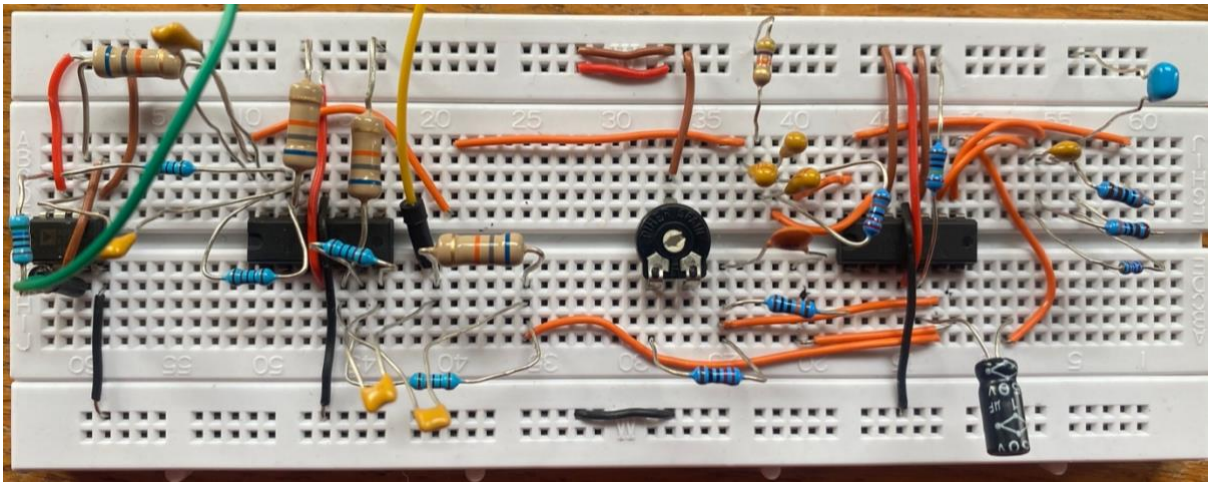

[Figure 4.2.16: Full EEG system with Vin from multiplexer logic (Red: +9V, Black: -9V, Brown: Ground, Yellow: Vout, Green: Vin]

With breadboard tests confirming the functionality of the simulations, the components were transferred over to a PCB. The first iteration of the PCB which was made during the design process. Edits were made however and a new PCB fabricated before assembly as explained below.

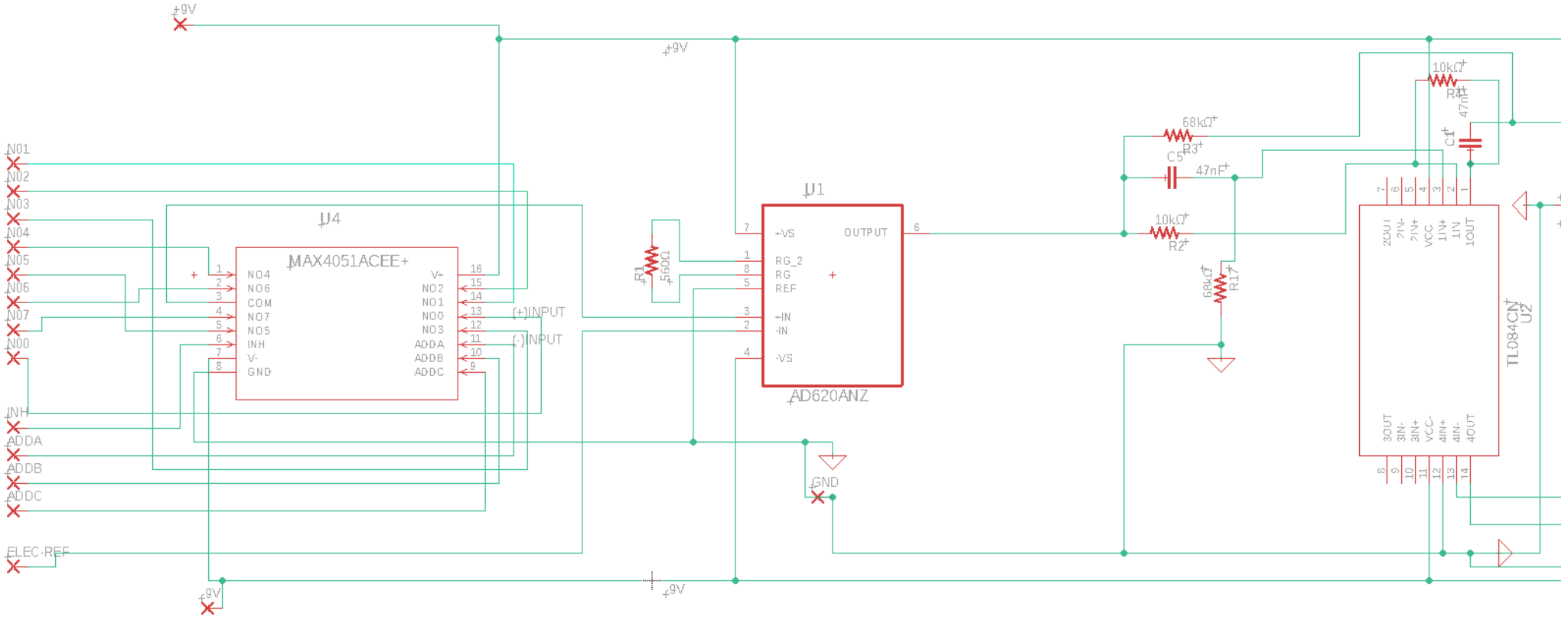

[Figure 4.2.17: PCB iteration 1, Circuit schematic of electroencephalogram electronics using Eagle software package]

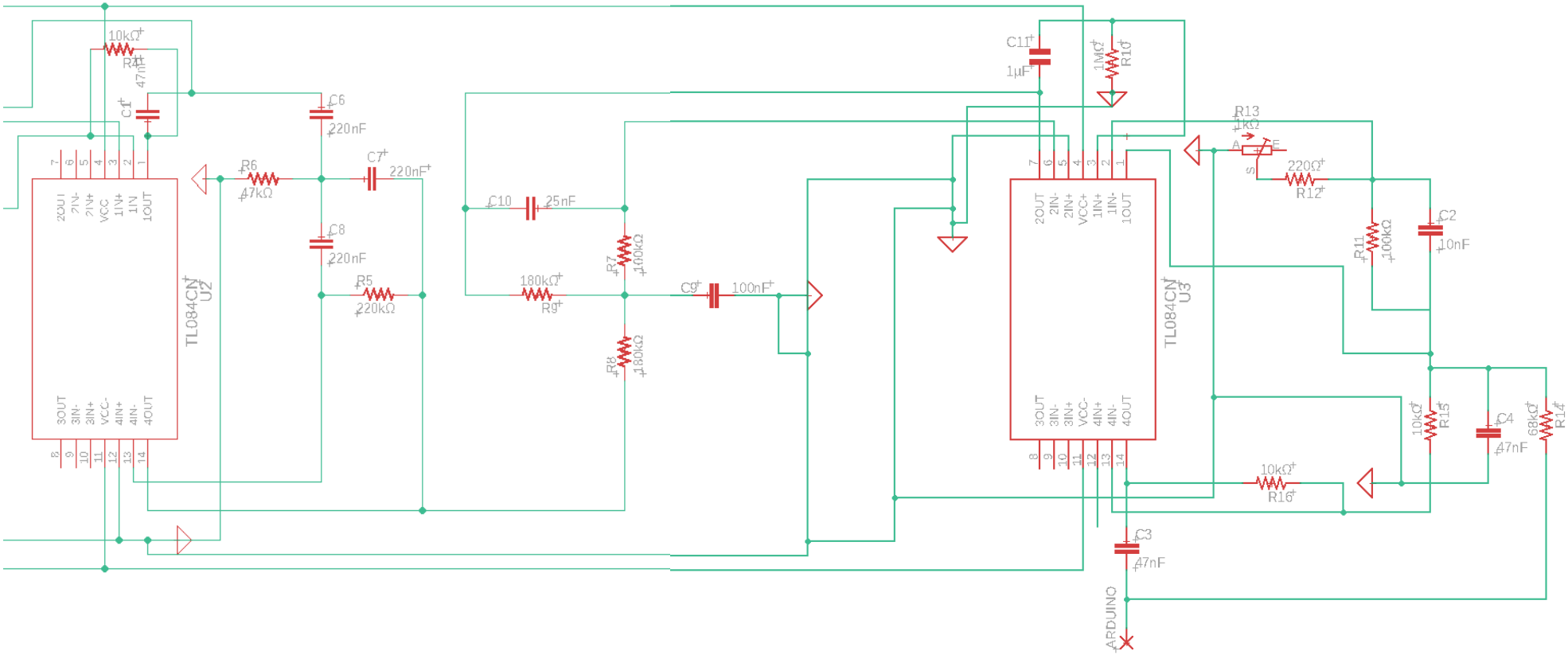

[Figure 4.2.17: PCB iteration 1, Circuit schematic of electroencephalogram electronics using Eagle software package]

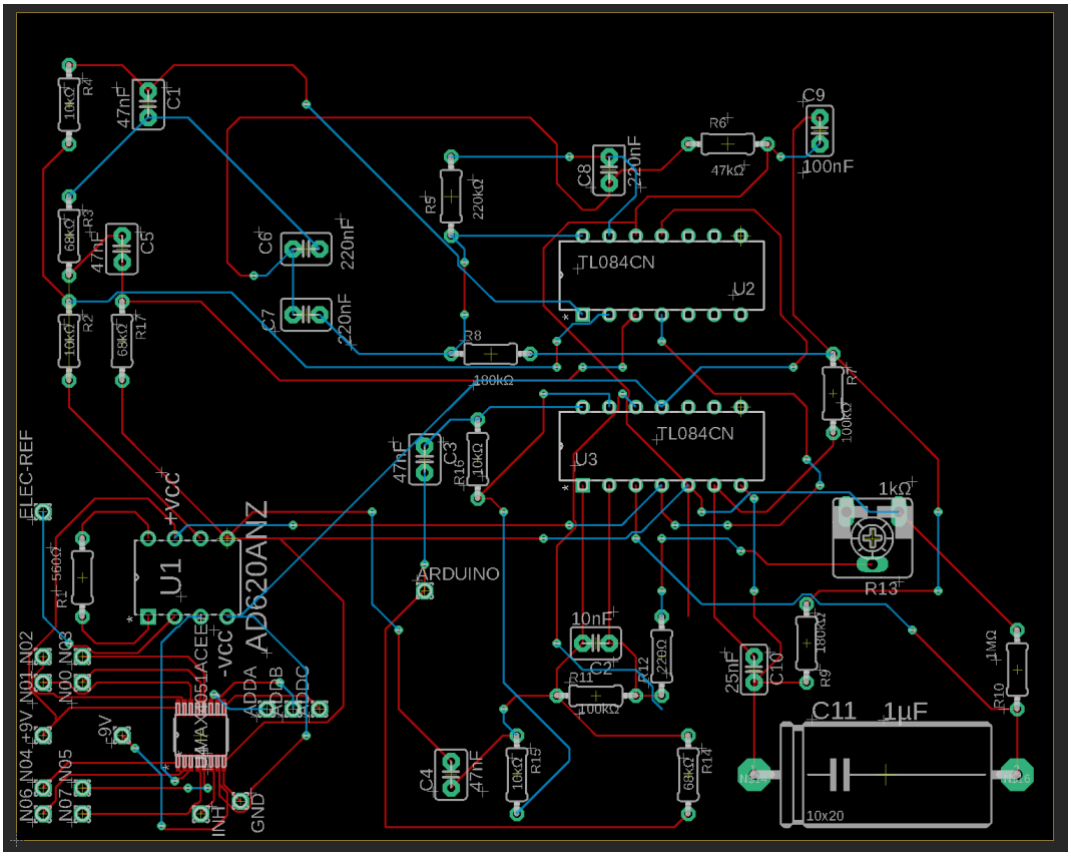

[Figure 4.2.18: Computer generated schematic of 100mm x 80mm electroencephalogram electronics PCB iteration 1. Layout of components and wiring paths]

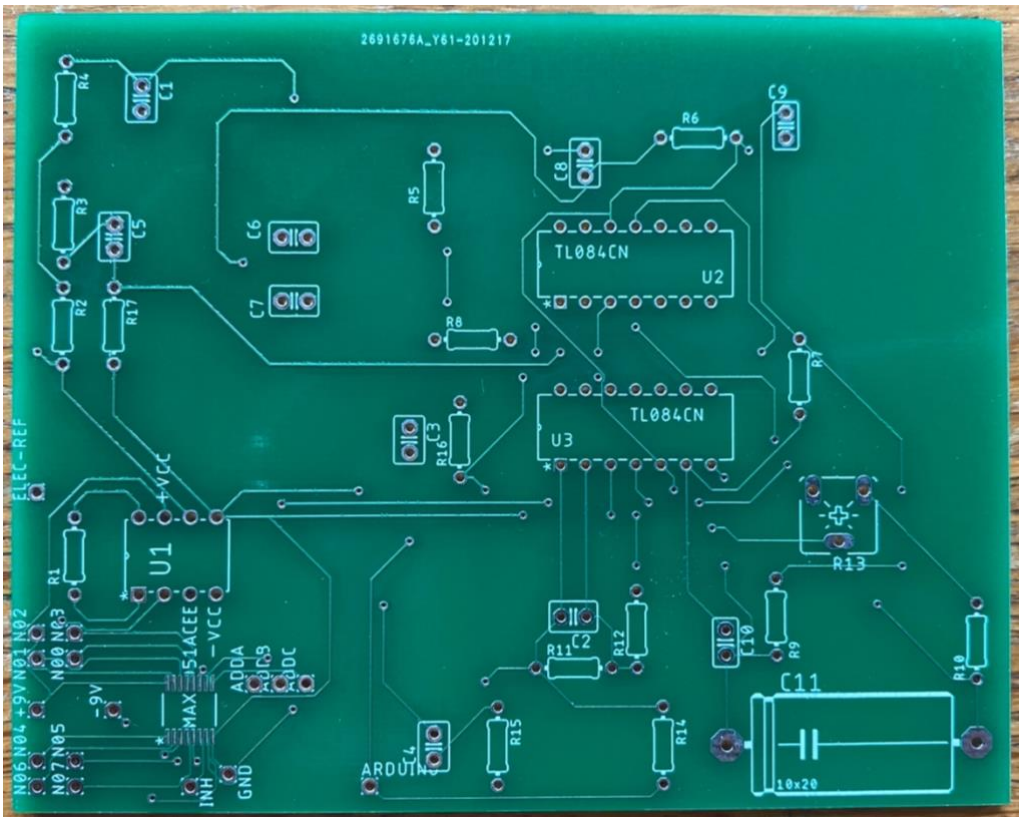

[Figure 4.2.19: Delivered board 100mm x 80mm electroencephalogram electronics PCB iteration 1. Layout of components and wiring path]

There were some issues with the original PCB design. Firstly, it was too large to mount on the cloth hat without potentially distorting the shape and ultimately moving the electrodes. Components in the circuit also changed during the design and testing phase which meant that an additional component was needed and the cut-out for C11 could be reduced in size. Some of the inputs into the multiplexer were also removed as they were redundant with only two control inputs. This allowed for a board which was less cluttered and thus helped to reduce the size down to 80mm x 60mm saving 8cm^2 from the area.

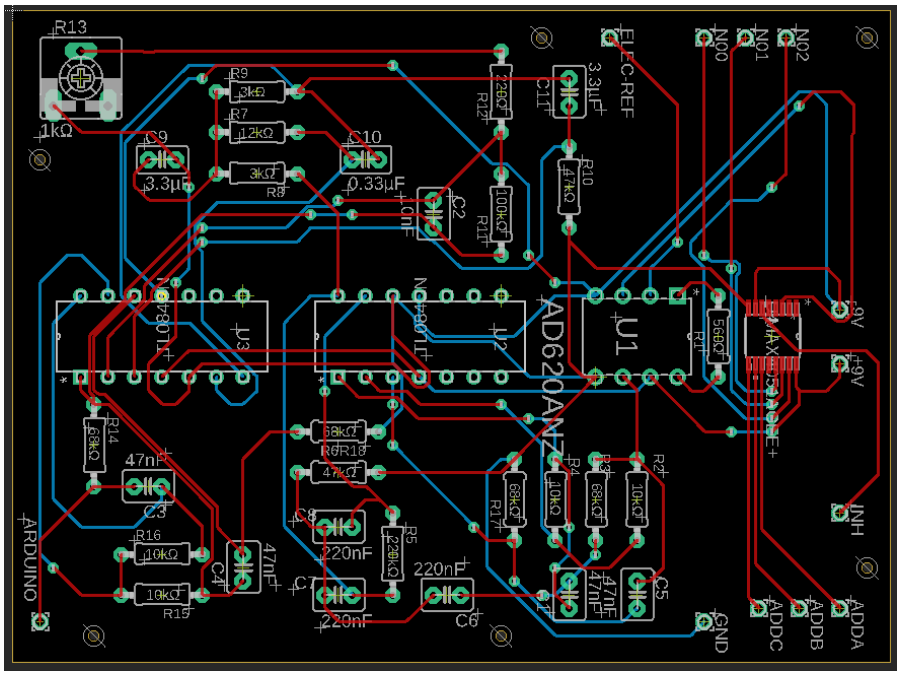

[Figure 4.2.20: Computer generated schematic of 80mm x 60mm electroencephalogram electronics PCB iteration 2. Layout of components and wiring paths]

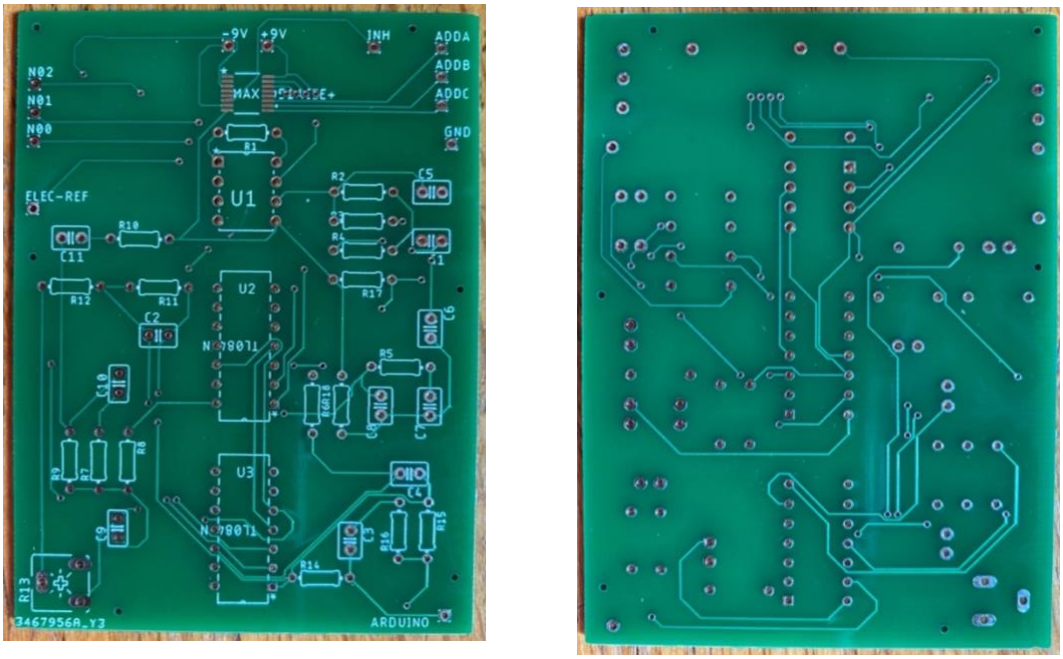

[Figure 4.2.21: Delivered board 80mm x 60mm electroencephalogram electronics PCB iteration 2. Layout of components and wiring path]

The second and final iteration of the schematic for the PCB can be seen in figure 4.2.22.

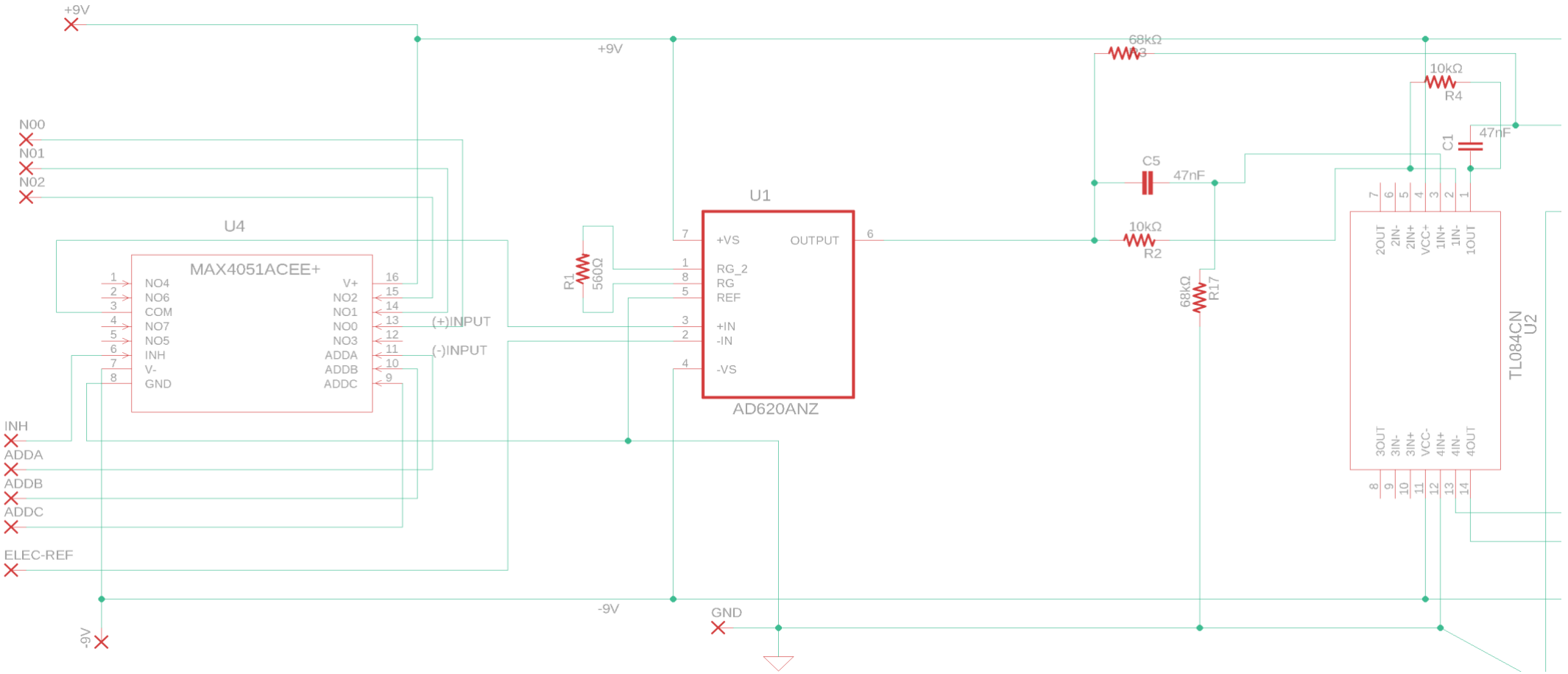

[Figure 4.2.22: PCB iteration 2, Circuit schematic of electroencephalogram electronics using Eagle software package]

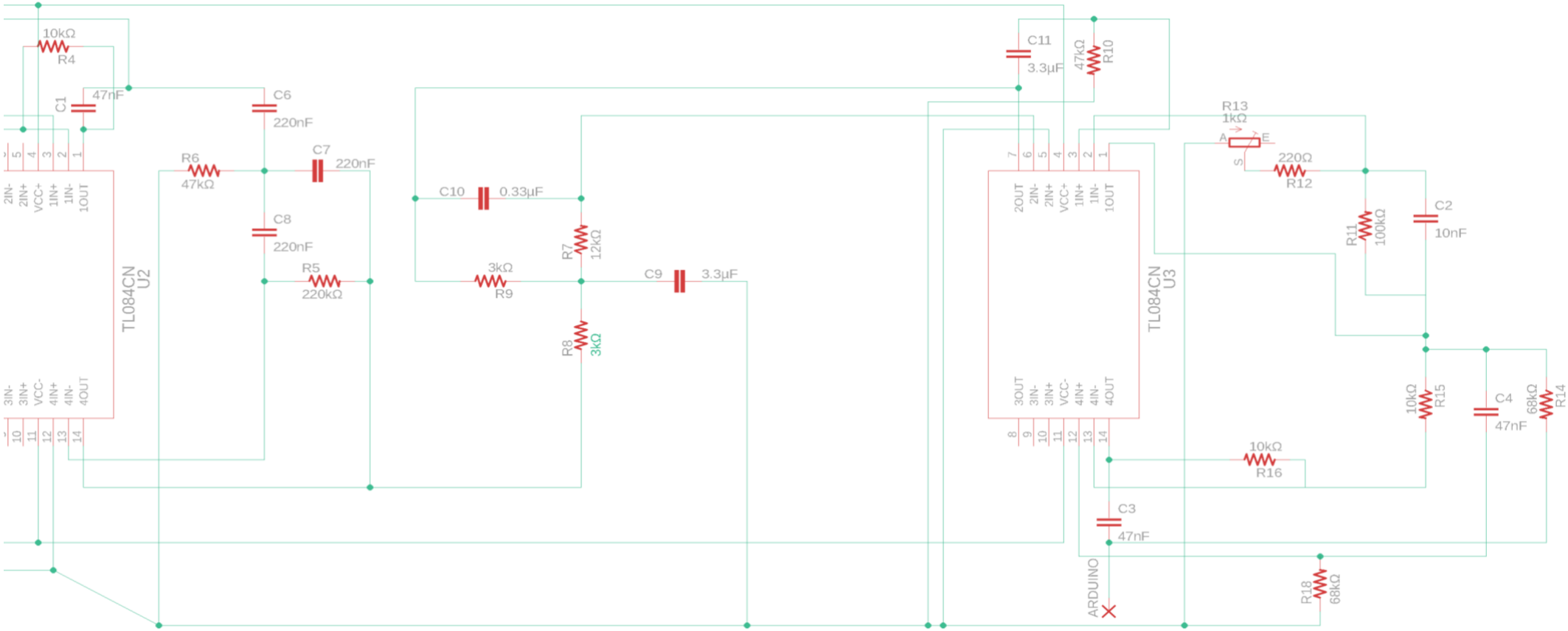

[Figure 4.2.22: PCB iteration 2, Circuit schematic of electroencephalogram electronics using Eagle software package]

Assembly

With the breadboard build completed and tested, the PCB was assembled. The components were soldered on following the schematics in figure 4.1.25.

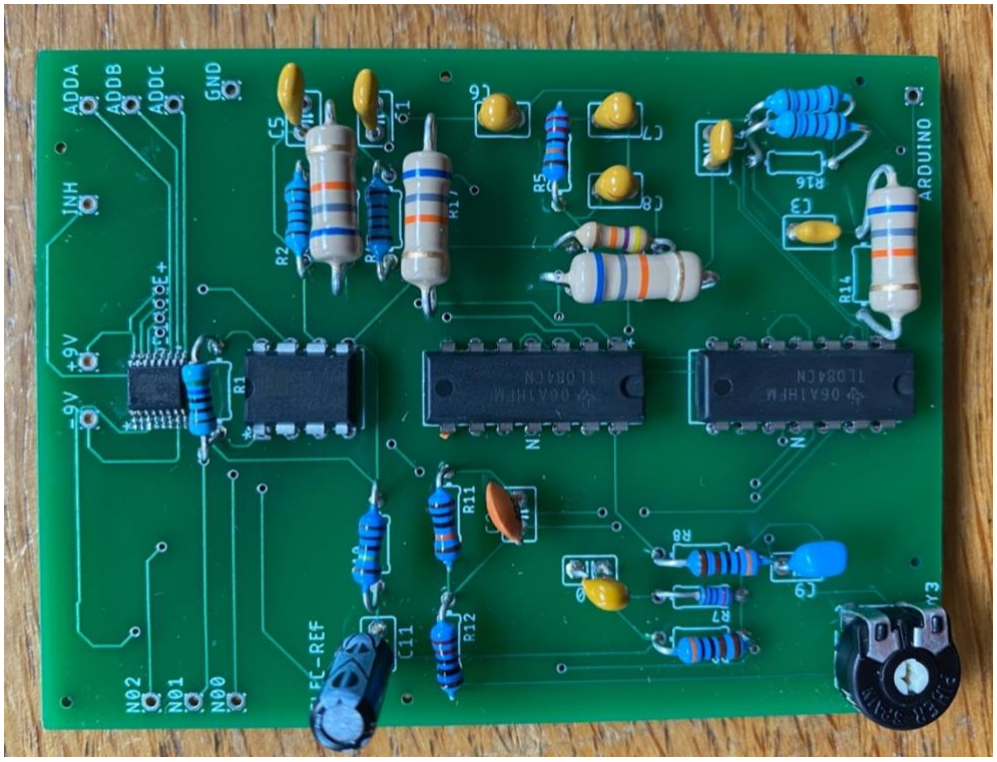

[Figure 4.2.23: assembly of electroencephalogram electronics onto PCB with components soldered on]

With the headset and electronics complete, the full hardware system was constructed. In order to save lost time some elements of the system where trimmed. Mounting the Elegoo on to the headset and having a separate power supply element were removed. The power supply suggested would, however, still work.

In order to select which input electrode connected to +Vin of the instrumental amplifier from the multiplexer an Arduino clone called an Elegoo Uno R3 was used. This microcontroller has the same functionality as the basic Ardunio but was more cost effective.

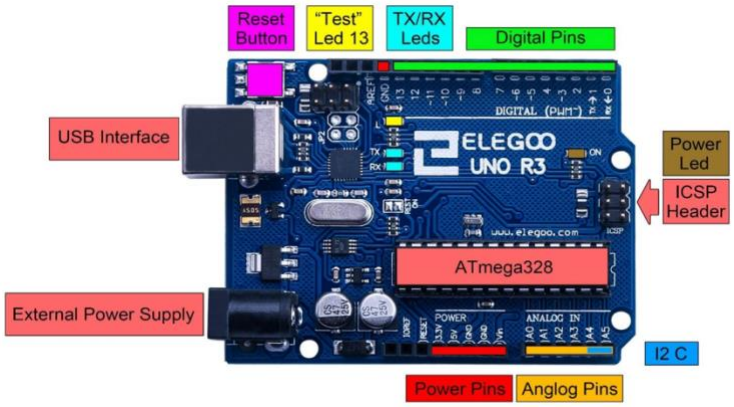

(ELEGOO, [32]) [Figure 4.2.24: Connection layout of the Elegoo Uno R3 based on the ATmega328 datasheet]

The electronics were connected to the Elegoo via the digital pins 6, 7, 12 and 13 as shown in the code (Figure A1/A2) within appendix A. The Elegoo was then connected to a laptop for uploading code and powering the Elegoo.

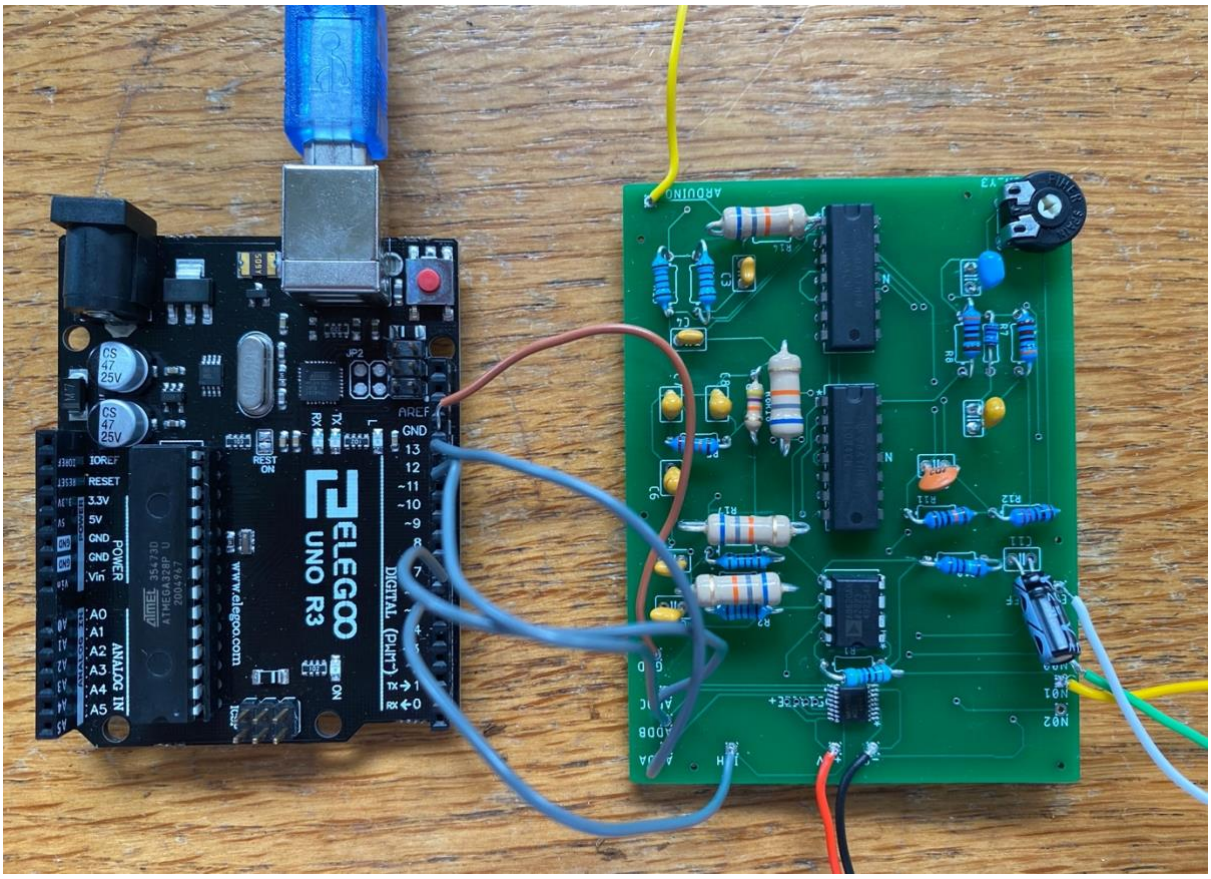

[Figure 4.2.25: Connections of encephalogram electronics to Elegoo (Wire colour: Gray), power supply (Wire colour: Red and Black), headset (Wire colour: White, Green & Yellow) and ground (brown). With Vout in Yellow]

4.3 Testing

With limited time remaining, the system was tested to confirm the functionality of the project by determining if activity from movement in a specific arm would show voltage fluctuations corresponding in time to when the limb was active.

In order to achieve this an oscilloscope was used with a probe connected to Vout and ground. The original multiplexer code was altered so that only the electrode from the left hemisphere of the motor cortex was activated constantly. This allowed a visual of the fluctuations in voltage output as movement from the right arm was performed. This can be seen in figure 4.3.3, over a period of 10 seconds.

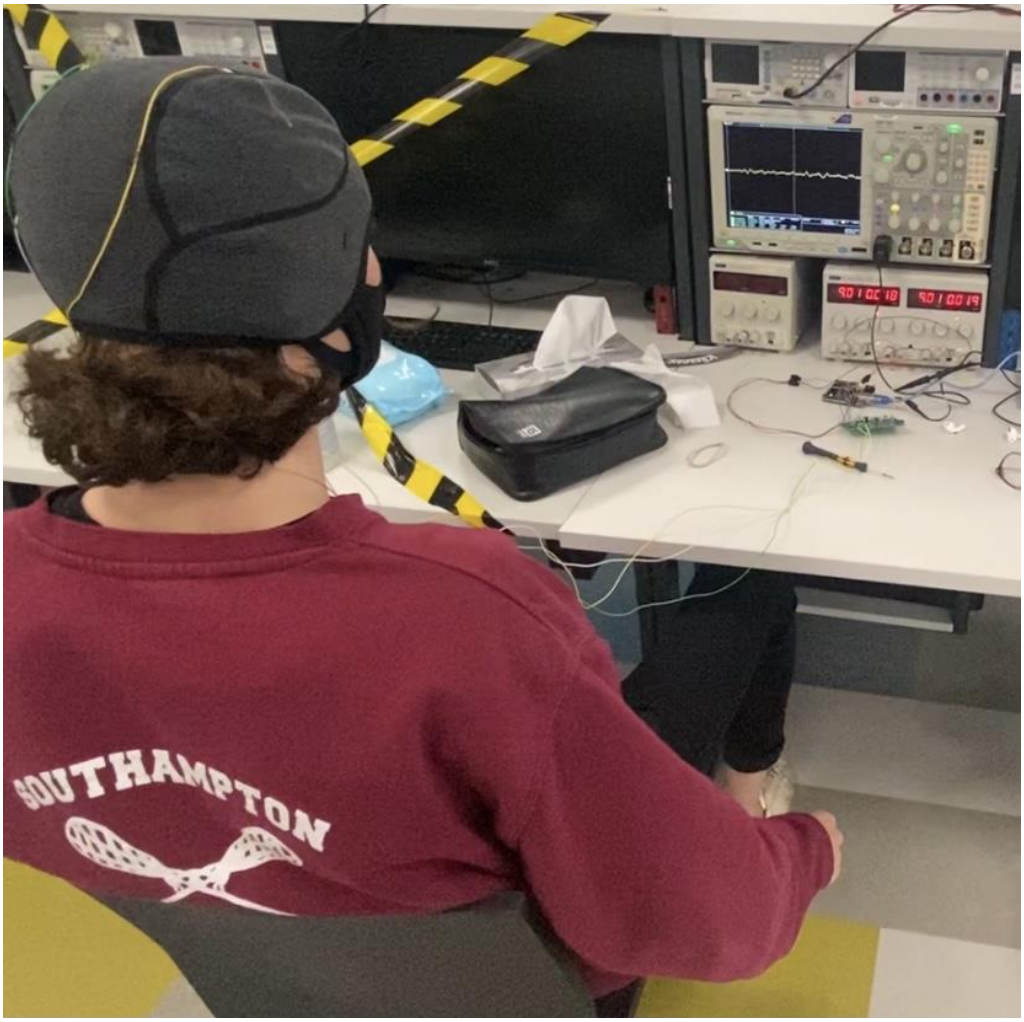

[Figure 4.3.1: System test with arm lateral to body at rest clearing mind to remove static fluctuation in base level voltage]

[Figure 4.3.2: System test with arm at 90 degrees to body and active showing voltage spikes due to motion]

Testing the electroencephalogram showed that changes in the level of concentration of the user would alter the stability of the base signal. A calmer state of mind yielded clearer differences between times when the motor cortex was active and at rest. This is due to higher levels of activity in the brain when concentrating resulting in larger noise on the electrode from neighbouring cortical regions and processes within the brain that use the motor cortex for processes. This can be seen in figure 3.5.2 when comparing the sleep and awake brain activity of a patient undergoing EEG testing.

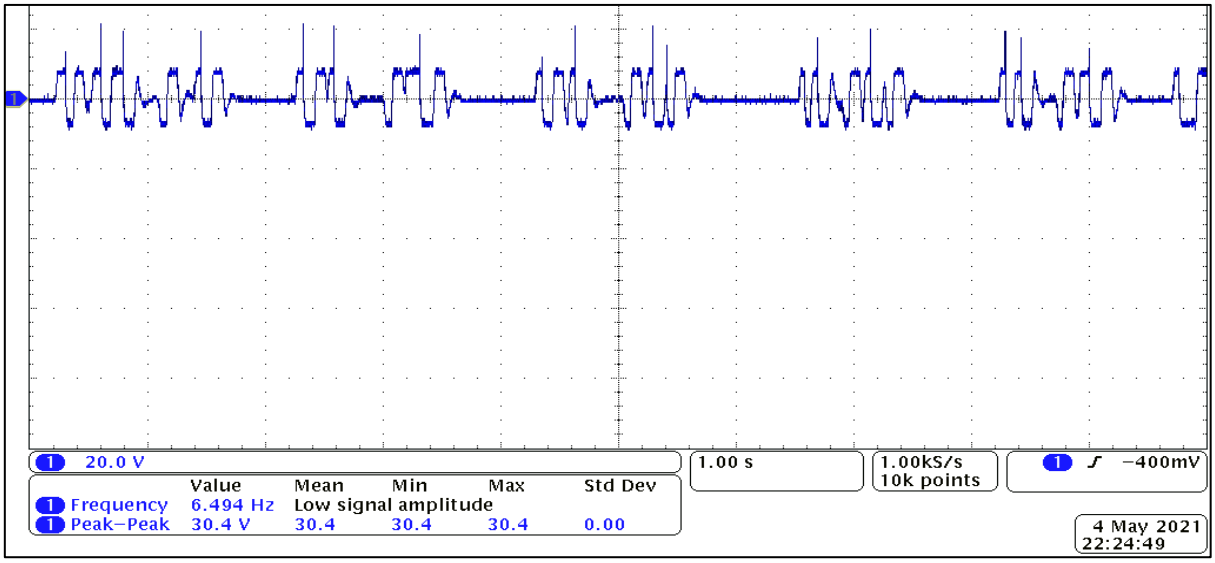

[Figure 4.3.3: Vout fluctuations over 10 seconds when the right arm is active. Time increment: 1 second per division, Voltage increment: 20V per division]

The right arm was moved laterally from an initial position at the waist to 90 degrees before being lowered. Voltage fluctuations were considerably larger when the muscles were active, moving the arm upward or downward. When relaxed the activity reduced significantly to a base level.

The values of voltage did however fall far outside the desired range of 0-1 volts. It is believed that the voltage range of data on the scalp from the motor cortex fluctuates more than originally expected when active compared to when at rest.

This issue could be resolved by increasing the resistance of the potentiometer within the non-inverting amplifier at R13. This would decrease the lower band of the gain to a more suitable value.

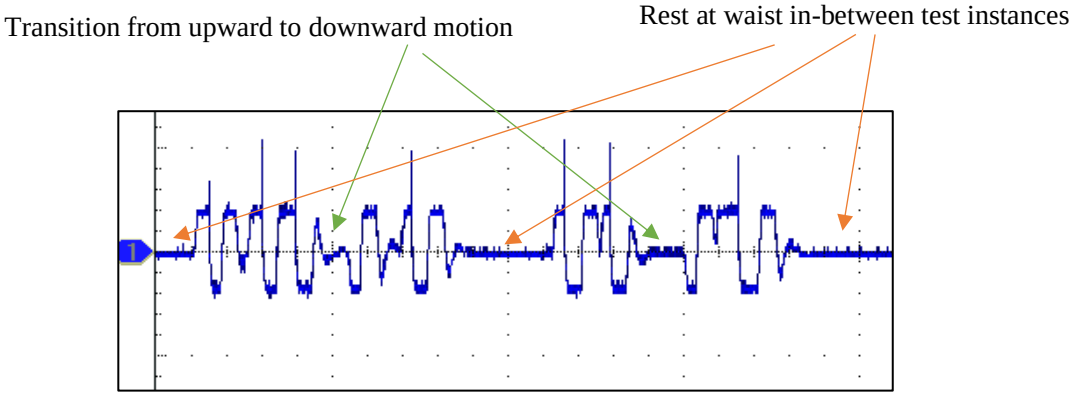

[Figure 4.3.4: Vout fluctuations when activating motor region under investigation. Horizonal time base 1 second per division, vertical voltage base 20 volts per division]

Movements of other muscle regions did not activate the voltage fluctuation showing that the result was purely from the activation in the right arm.

Chapter 5: Project Evaluations & Further Work

Using the literature, a system was designed and built which successfully detected the moments of the arm as fluctuations in output voltage from the encephalogram. The paper establishes the elements of the brain and their purpose, providing detail into how electrical signals can be read from the scalp and where to place the electrodes. Using this information an encephalogram was created with steps to achieving the same results shown in detail. With the system constructed an output was achieved that provided a proof of concept for the potential to create an operational control system.

Further work would include resolving the issue of the output voltage amplitude as stated in chapter 4.3 ‘Testing’. It would also include writing a post processing program to extract the specific frequencies within the signals. These specific frequencies would provide a more accurate way of detecting the movement in a given cortical region by generating ‘signatures’ for each motor region corresponding to a cluster of frequencies to be used as a switch. A fast Fourier transform or FFT is useful mathematical operation for this process.

Chapter 6: Project Management

6.1 Time Management

Given that this was the first largescale project for myself and the unique nature of this year, time management was an area constantly developed throughout the project. The covid epidemic has affected nearly every facet of life making it of paramount importance to work through the project with a solid management system in place, capable of adapting to the changes in availability of access to labs and other elements of the project.

Agile project management has been used in software development for some time and given the need for adaptability it was implemented here. Simply put, the agile system follows a design, development (build) and test model which loops until the task is complete. This can be seen below,

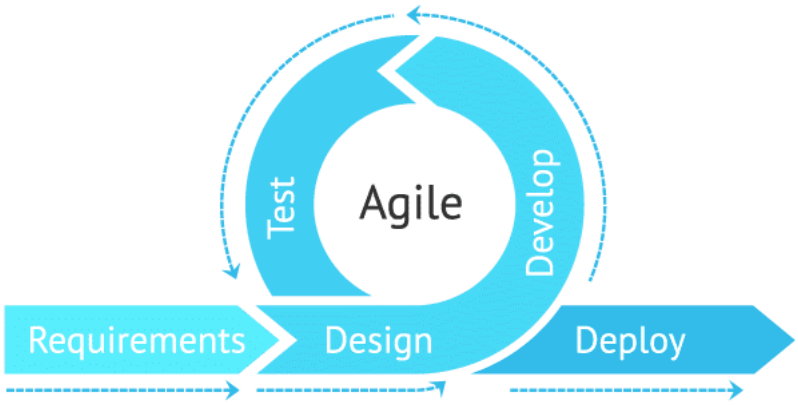

(Goff, 05.03.21 [28]) [Figure 6.1.1: Agile project management workflow diagram]

The key aspect of this system was that tasks are completed in parallel instead of sequentially. During the academic year the country has been placed in two national lockdowns, with rules specifically for universities changing more frequently than that. This meant access to labs would be cut off for indeterminant lengths of time. To limit this issue, tasks were naturally taken on in pairs with research, coding and initial design not needing such facilities while the technical progress hinged on lab access for simulations, testing and the build.

The first iteration of the Gant chart was made before this system was implemented at the start of the academic year. Revisions were completed when the interim report was submitted in early December. A final version was made in March when the labs were scheduled to open.

This final stage was also largely affected by a personal medical operation scheduled for mid-March which involved 2 weeks of isolation before and after the surgery. This unfortunately coincided with labs opening, thus reducing the overall time of lab access.

Within all of the Gant chart iterations the weeks represented in darker grey (with white text) are there to show an inability to access the labs for the following reason.

- Closer due to holiday.
- Closer due to COVID-19 and the subsequent government guidelines regarding university access.
- Isolation due to awaiting a scheduled surgery.

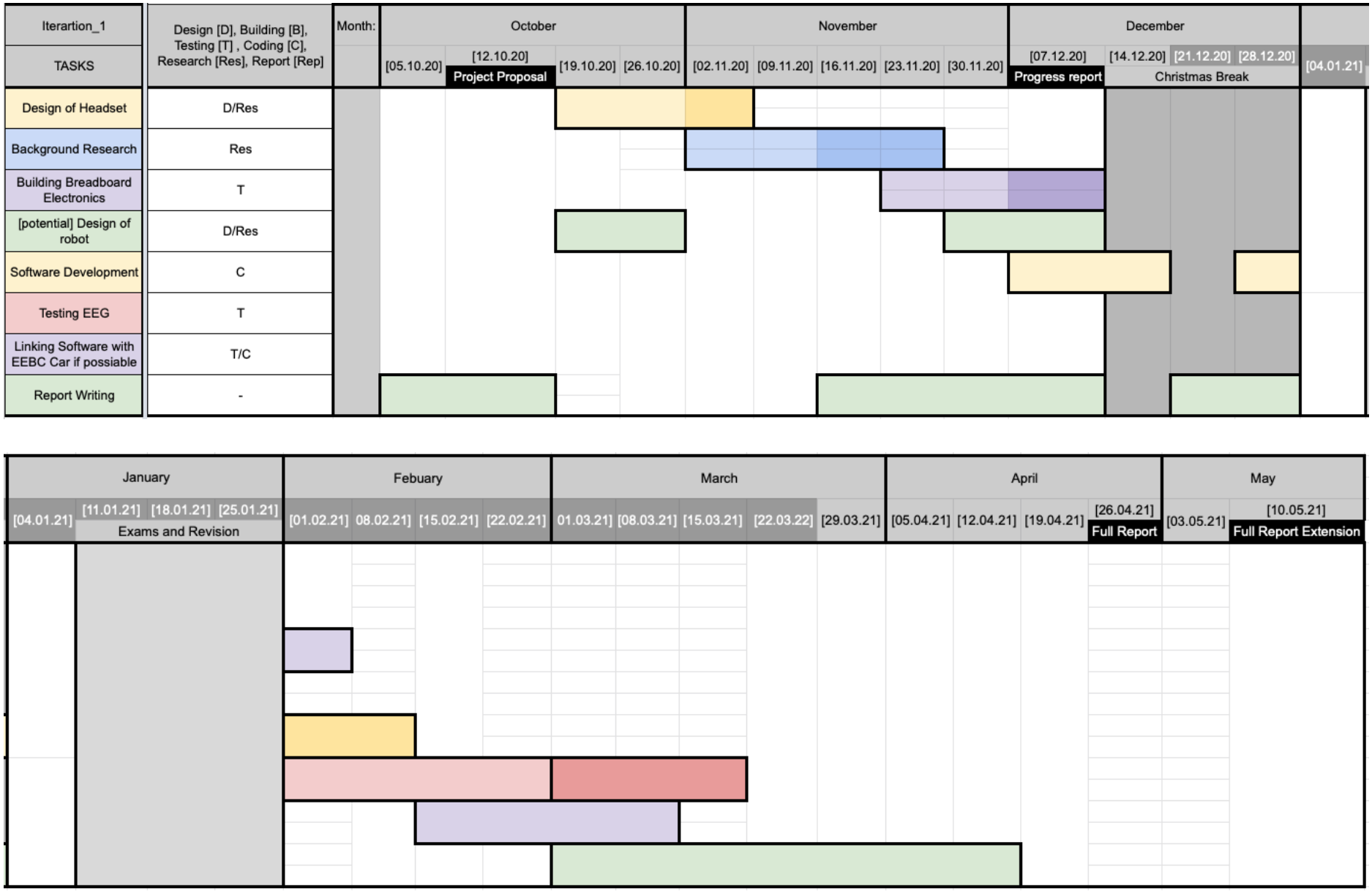

[Figure 6.1.2: Gant Chart iteration 1 of workflow for the academic year, created during the beginning of the project]

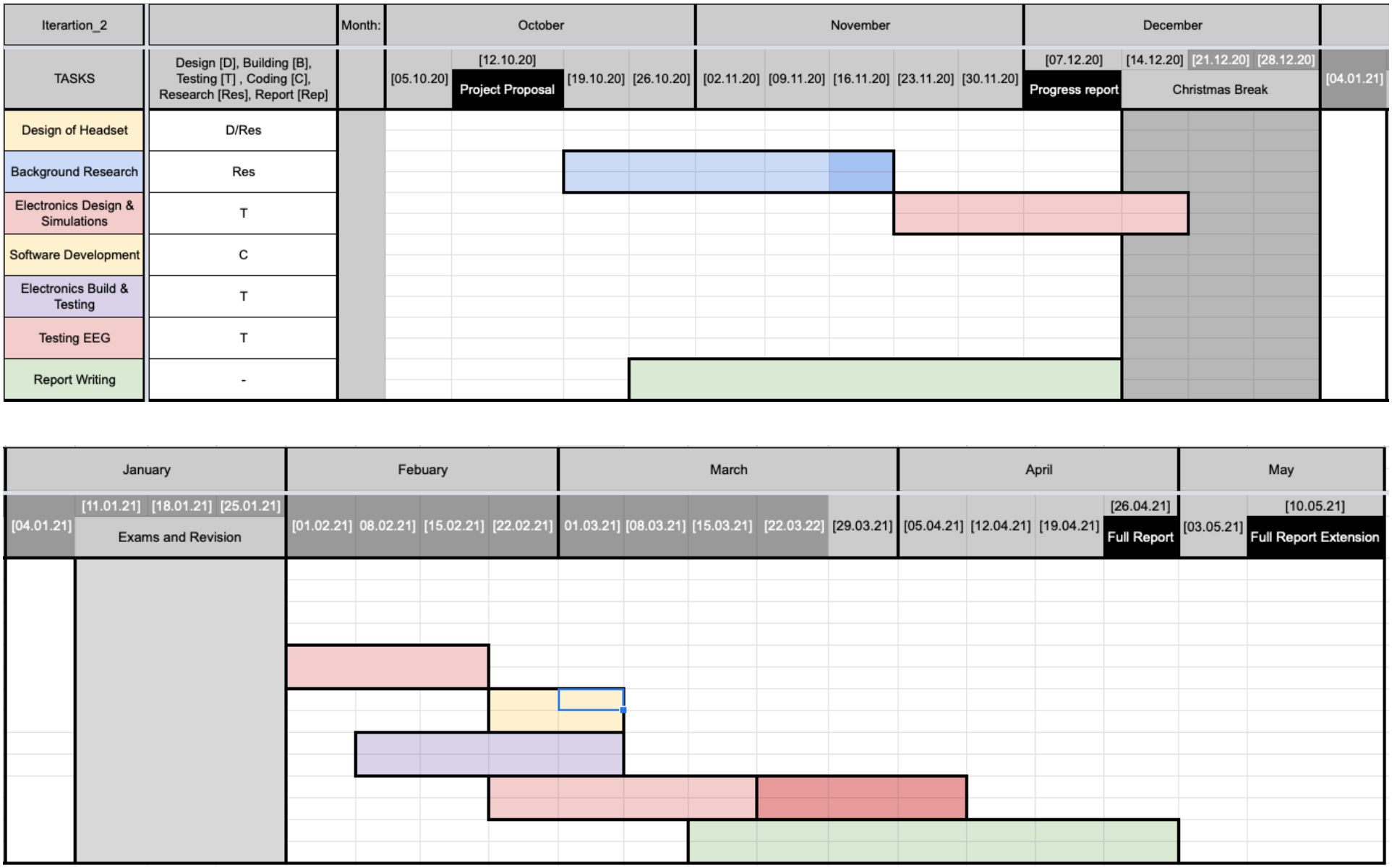

[Figure 6.1.3: Gant Chart iteration 2 of workflow for the academic year, laid out during end of winter term and interim submission]

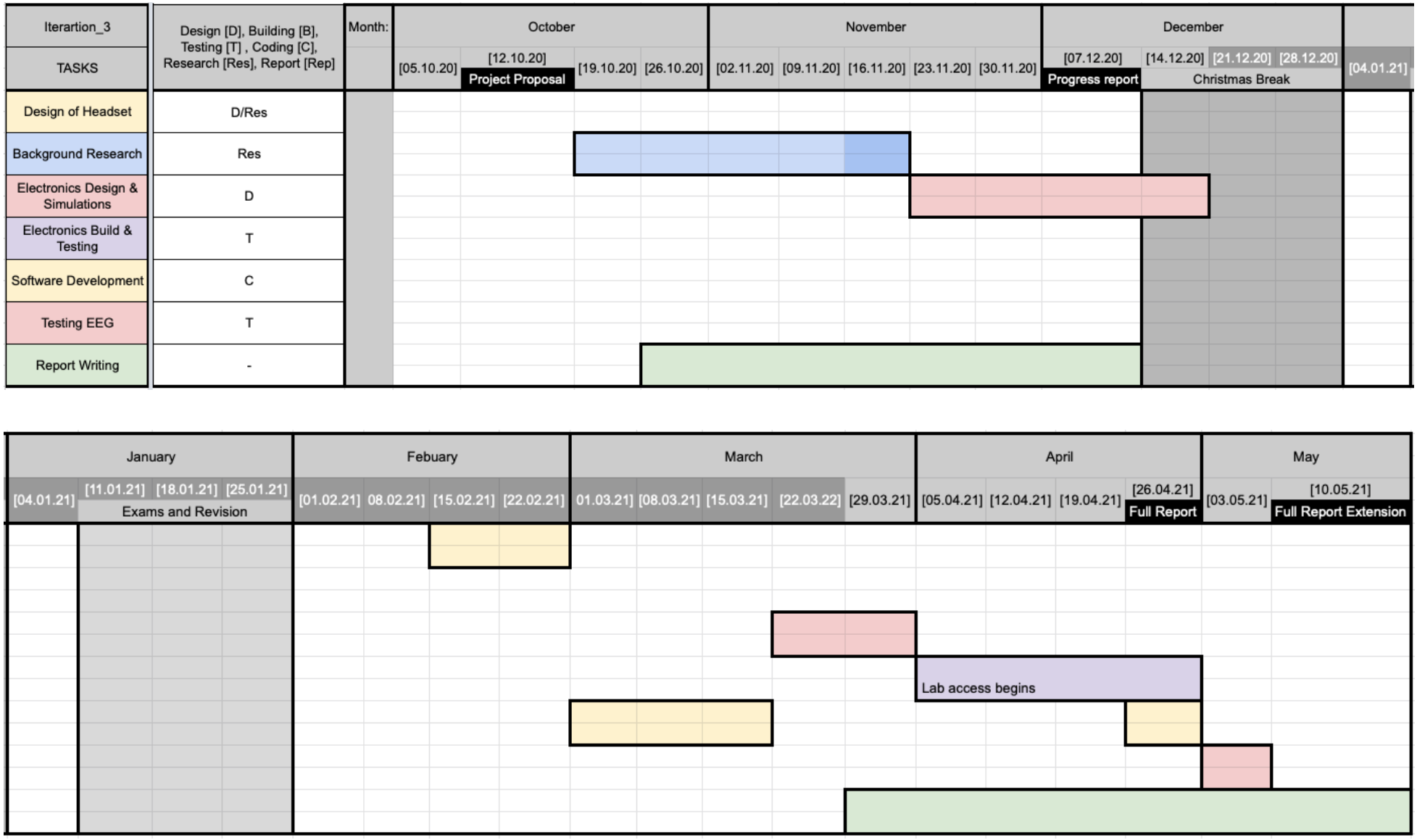

[Figure 6.1.4: Gant Chart iteration 3 of workflow for the academic year, laid out when lab work began – accurate to week of specific work completed]

5.2 Risk Management

Important in any project is the ability to circumvent issues that will likely arise during the year. A system was put into place for this reason. This consisted of identifying risks associated with the project, work involved or personal events. The damage that would be caused by each event is established with individual responses made accordingly. The likelihood and significance are also established within the risk matrix below.

	Risk	Effects	Potential for Minimising Damage
1	Illness [Covid or otherwise]	Delay to work-flow.	Follow goverments guidlines on COVID-19 and avoid unncessary contact with involiduals outside the house when instucted to.
2	Planned operation [Date not confimed]	3/4 Weeks of isolation. No access to labs if open	Once infomed of the date, imidialy adjust and reorganise work-flow to target tasks not requiring the labs.
3	Componet Delay	Delay to work-flow. Potentially unable to continue with lab work	Order in advance while being consise on when ideas are planned for use.
4	Over Budget	Limiting the project reach, while requesting for finacial extension	Make clear, calcuated descions about what to purchase and it neccesity to the project. Items for design should be checked several times.
5	Loss of data [Reports/ Figures]	Delay to work flow while repeating experiments or rewriting element of report	Save copies of each iterstion of the report and any model made. Logic filing system will reduce chance of getting lost before being adding into report
6	Closure of Labs	Doing complex simulations wont be possible with the univeristy software on my mac. Testing heavily requires lab oscilloscope and signal generator	Try to adapt project where possible. Reduce complexity of the robot being used for contol would save lab time.
7	Modules outside of project	To much time allocated to either will result in uncomplete work, stress and ultimatly worse grades	More enforcies on agile time managment system. Work on modules more priod to exam periods and when labs are closed

[Table 6.2.1: Tables of issues potentially damaging to the project progress]

Probability	Consquances				
	Insignificant	Low	Medium	High	Significant
Serve		1		2	6
Major		3			
Moderate			4/7		5
Minor					
Minimal					

[Table 6.2.2: Risk matrix for issues potentially damaging to the project progress]

6.3 Budget Management

The project followed a strict budget of £150 for all elements. In order to remove the chance of overspending the project budget was reduced to £100 with £50 remaining to buy any elements that either needed replacing due to design error or component faults. Costs were also reduced by taking advantage of the available equipment at the university labs. This covered the majority of the capacitor and resistor components.

A full list of the components and where they were purchased can be seen in table 5.3.1 along with an overall cost. Table 5.3.1 shows the components purchased within original £100 budget goal and Figure 5.3.2 shows any replacement components with the remaining £50.

Electroencephalographic Headset:	Qt	Compent	Supplier	Product Code	Mft. Part No.	Cost	Avaliable from Lab	Items Ordered
Base	1	Skill Cap	Amazon	-	-	£ 9.99	☐	☑
		PCB	-	-	-	£ 18.00	☐	☑
Resistors	1	1 kΩ (Potentiometer)	Lab	-	-	-	☑	☐
	1	220 Ω	Lab	-	-	-	☑	☐
	1	560 Ω	Lab	-	-	-	☑	☐
	4	10k Ω	Lab	-	-	-	☑	☐
	1	47k Ω	Lab	-	-	-	☑	☐
	1	100 kΩ	Lab	-	-	-	☑	☐
	2	3 kΩ	Lab	-	-	-	☑	☐
	1	12 kΩ	Lab	-	-	-	☑	☐
	1	220 kΩ	Lab	-	-	-	☑	☐
	4	68k Ω	Lab	-	-	-	☑	☐
	1	1 MΩ	Lab	-	-	-	☑	☐
Capacitors	1	10 nF, Ceramic	Lab	-	-	-	☑	☐
		3.3 µF, Ceramic	Lab	-	-	-	☑	☐
		330 nF, Ceramic	Onecall	**9708480**	**MCCB1V104M2ACB**	£ 1.18	☐	☑
	3	220 nF, Tantalum	Onecall	**2852757**	**TAP224K035SRW**	£ 3.37	☐	☑
	1	1 µF, Electrolytic	Lab	-	-	-	☑	☐
	4	47nF, Ceramic	Lab	-	-	-	☑	☐
Chips	1	8:1 Multiplexer MAX4051ACEE+	Onecall	**2513682**	**MAX4051ACEE+**	£ 1.93	☐	☑
	1	Instrumetation Amplifer - AD620AN	Onecall	1079404	**AD620ANZ**	£ 11.62	☐	☑
	2	Quad Op-Amp - TL084CN	Onecall	**3117825**	**TL084CN**	£ 0.90	☐	☑
PSU	2	9v Batteries	-	-	-	-	☑	☐
	1	Battery pack holster	-	-	-	-	☑	☐
Controller	1	ELEGOO Uno R3	Amazon	-	-	£ 13.58	☐	☑
Conductive Gel	1	Electrode Gel, 16oz (473ml)	Unimed	E9		£ 15.00	☐	☑
Cups	10	10mm Disp Cup Electrode, 150cm lead	Unimed	DAGD152600/ 25	-	£ 11.70	☐	☑
Delivery	-	-	-	-	-	£ 15.00	☐	☑
					Total cost	£ 102.26		

[Table 6.3.1: Parts list and costs sheet for original £100 estimated budget]

Electroencephalographic Headset:	Qt	Compent	Supplier	Product Code	Mft. Part No.	Cost	Avaliable from Lab	Items Ordered
		PCB	-	-	-	£ 18.00	☐	☑

[Table 6.3.2: Replacement parts list and costs sheet for £50 estimated remaining budget]

Due to errors found in the original PCB design a new board was fabricated as explained within the build on page 52. This was the only element replaced and so the total costs were within budget at £120.26 (80%).

Bibliography

[1]. Abiyev, R. H., Akkaya, N., Aytac, E., Gunsel, I., & Cagman, A. (2016). Brain-Computer Interface for Control of Wheelchair Using Fuzzy Neural Networks. *BioMed Research International, 2016*. https://www.hindawi.com/journals/bmri/2016/9359868/

[2]. Analog Devices. (2003 -2011). *Low Cost Low Power Instrumental Amplifier*. Analog Devices. https://www.analog.com/media/en/technical-documentation/data-sheets/AD620.pdf

[3]. Azvolinsky, A. (2018, October 8). *Both Sides of the Brain Are Active During One-Sided Arm Movement*. The scientist exploring life inspiring innovation. https://www.the-scientist.com/news-opinion/both-sides-of-the-brain-are-active-during-one-sided-arm-movement-64909

[4]. Belkacem, A. N., Saetia, S., Zintus-art, K., Shin, D., Kambara, H., Yoshimura, N., Berrached, N., & Koike, Y. (2015, November 15). Real-Time Control of a Video Game Using Eye Movements and Two Temporal EEG Sensors. *Computational Intelligence and Neuroscience, 2015*(Article ID 653639). https://doi.org/10.1155/2015/653639

[5]. Biga, L. M., Dawson, S., Harwell, A., Hopkins, R., Kaufmann, J., LeMaster, M., Matern, P., Morrison-Graham, K., Quick, D., & Runyeon, J. (2002). Nervous Tissue. In *Anatomy & Physiology*. Oregon Stage University. https://open.oregonstate.education/aandp/chapter/12-2-nervous-tissue/

[3]. Bos, D. O. (2006). The Influence of Visual and Auditory Stimuli. In *EEG-based Emotion Recognition* (pp. 1-17). University of Twente.

[6]. Bright, D., Nair, A., Salvekar, D., & Bhisikar, S. (2016). EEG-based brain controlled prosthetic arm. In *Conference on Advances in Signal Processing (CASP)* (pp. 479-483). IEEE Xplore. https://ieeexplore.ieee.org/document/7746219/citations#citations

[7]. Bundy, D. T., Szrama, N., Pahwa, M., & Leuthardt, E. C. (2018, November). Unilateral, 3D Arm Movement Kinematics Are Encoded in Ipsilateral Human Cortex. *The Journal of*

Neursoscience, 38, 10042-10056. https://www.jneurosci.org/content/38/47/10042/tab-figures-data

[8]. cah6. (2012, June 22). *DIY EEG (and ECG) Circuit*. Instructables. https://content.instructables.com/pdfs/E0Q/PSBM/H3QFIZG7/DIY-EEG-and-ECG-Circuit.pdf

[9]. Campbell, I. G. (2019). EEG recording and analysis for sleep research. In Curr Protoc Neurosci (Vol. Chapter 10). PMC. https://www.ncbi.nlm.nih.gov/pmc/articles/PMC2824445/

[10]. Davidson, M. C., Amso, D., Anderson, L. C., & Diamond, A. (2006, March 31). Development of cognitive control and executive functions from 4 to 13 years: Evidence from manipulations of memory, inhibition, and task switching. Neuropsychologia, 44(11). https://www.ncbi.nlm.nih.gov/pmc/articles/PMC1513793/

[11]. Deusen, M. V. (2019, December 12). REM Sleep: What is It, Why it's Important, How Much You Need & How to Increase It. WHOOP. https://www.whoop.com/thelocker/what-is-rem-sleep/

[12]. The Human Memory. (2020, November 25). Sensory Cortex. The Human Memory. https://human-memory.net/sensory-cortex/

[13]. Jennes, L. (2017). Cytology of the Central Nervous System. In Conn's Translational Neuroscience. Academic Press. https://www.sciencedirect.com/topics/neuroscience/unipolar-neuron

[14]. Khanna, A. (2020, May 25). Action potential. TeachMePhysiology. https://teachmephysiology.com/nervous-system/synapses/action-potential/

[15]. Kovac, G. G. (2018). Neuropathology. In Handbook of Clinical Neurology (Vol. 145, pp. 13-23). Elsevier. https://www.sciencedirect.com/topics/neuroscience/unipolar-neuron

[16]. Machado, S., Araujio, F., Paes, F., Velasques, B., Cunha, M., Budde, H., Basile, L. F., Anghinah, R., Arias-Carrion, O., Cagy, M., Piedade, R., de Graaf, T. A., Sack, A. T., & Ribeiro,

P. (2010). EEG-based brain-computer interfaces: an overview of basic concepts and clinical applications in neurorehabilitation. Reviews in the neuroscience, 21(6). https://pubmed.ncbi.nlm.nih.gov/21438193/

[17]. MAXIM. (2005). Low-Voltage, CMOS Analog Multiplexers/Switches (Rev 2 ed.). MAXIM. https://pdfserv.maximintegrated.com/en/ds/MAX4051-MAX4053A.pdf

[18]. Mok, K. (2017, January 22). How to Control a Robotic Arm with Your Mind, by Using Machine Learning. THENEWSTACK. https://thenewstack.io/control-robotic-arm-mind-using-machine-learning/

[19]. OKAWA. (2004). Filter design and Analysis. http://sim.okawa-denshi.jp/en/Fkeisan.htm

[20]. Connie Rye, Robert Wise, Vladimir Jurukovski, Jean DeSaix, Jung Choi, Yael Avissar . (2016, Oct 21). Biology, Openstax

https://openstax.org/books/biology/pages/1-introduction

[19]. Reif, P. S., Strzelczyk, A., & Rosenow, F. (2016, April 13). The history of invasive EEG evaluation in epilepsy patients. Epilepsy Center Hessen and Department of Neurology, 191-194. https://www.seizure-journal.com/article/S1059-1311(16)30022-X/pdf

[20]. Salvetti, A., & Wilamowski, B. M. (2008). A Brain-Computer Interface for Recognizing Brain Activity. In (pp. 714 - 719). IEEE Xplore. https://www.researchgate.net/publication/4356752_A_brain-computer_interface_for_recognizing_brain_activity

[21]. Smith, S. J. M. (2005). EEG in neurological conditions other than epilepsy: when does it help, what does it add? Journal of Neurology Neurosurgery and Psychiatry, 12(8).

[22]. Smith, S. J. M. (2005, June 16). EEG in the diagnosis, classification, and management of patients with epilepsy. Neurology, Neurosurgery & Psychiatry, 76(2). https://jnnp.bmj.com/content/76/suppl_2/ii2

[23]. Stefen, H., Ben-Menachem, E., Chauvel, P., & Guerrini, R. (2012, December). Case Studies into Epilepsy - Diagnosis. Cambridge University Press.

https://www.cambridge.org/core/books/case-studies-in-epilepsy/diagnosis/E67D8DEBDB884869D31AB64B0A1EA45A

[23]. Stone, J. L., & Hughes, J. R. (2013, February). Early History of Electroencephalography and Establishment of the American Clinical Neurophysiology Society. Journal of Clinical Neurophysiology, 30(1).

[24]. Sutton, S. (2018, June 5). Homunculus Map. fineartamerica. https://fineartamerica.com/featured/homunculus-map-spencer-sutton.html

[25]. Szymik, B. (May 9, 2011). What Are the Regions of the Brain and What Do They Do? Arizona State University School of Life Sciences Ask A Biologist. https://askabiologist.asu.edu/brain-regions

[26]. Texas Instruments. (2020). TL08xx FET-Input Operational Amplifiers. Texas Instruments. https://www.ti.com/lit/ds/symlink/tl084.pdf?HQS=TI-null-null-mousermode-df-pf-null-wwe&ts=1606893675191&ref_url=https%253A%252F%252Fwww.mouser.it%252F

[27]. The Albert Team. (2020, July 22). Afferent vs. Efferent: What's the Difference? AP® Psychology Crash Course Review. AP Psychology. https://www.albert.io/blog/afferent-vs-efferent-whats-the-difference-ap-psychology-crash-course-review/

[28]. Addy Goff. (05.03.2021). What is agile methodology in project management. Hive. https://hive.com/blog/what-is-agile-project-management-methodology/

David Bundy, Eric Leuthardt (2011) An EEG-Based interface for rehabilitation and restoration of hand control following stoke using ipsilateral cortical physiology. https://pubmed.ncbi.nlm.nih.gov/22255773/

[30]. Abdelkader Nasreddine Belkacem, Supat Saetia, Kalanyu Zintus-art, Duk Shin, Hiroyuki Kambara, Natsue Yoshimura, Nasreddine Berrached and Yasuharu Koike. Academic editor: Peitro Acrico Vol 2015. Real-Time control of a video game using eye movements and two temporal EEG sensors. https://www.hindawi.com/journals/cin/2015/653639/

[31]. Jianjun Meng, Shuying Zhang, Angeliki Bekyo, Jaron Olsoe, Bryan Baxter & Bin He (14 December 2016) Non-invasive electroencephalogram-based control of a robotic arm for reach and grasp tasks. https://www.nature.com/articles/srep38565

[32]. ELEGOO UNO R3 Data sheet https://epow0.org/~amki/car_kit/Datasheet/ELEGOO%20UNO%20R3%20Board.pdf

[33]. Biology 2e. Provided by: OpenStax. Located at: http://cnx.org/contents/185cbf87-c72e-48f5-b51e-f14f21b5eabd@10.8. License: CC BY: Attribution. License Terms: Access for free at https://openstax.org/books/biology-2e/pages/1-introduction

Appendix A: Code base

Multiplexer

```
int INH = 6;
int ADDA = 7;
int ADDB = 12;
int ADDC = 13;

void setup() {
pinMode(ADDA, OUTPUT);
pinMode(ADDB, OUTPUT);
pinMode(ADDC, OUTPUT);
pinMode(INH, OUTPUT);
}

void loop()
{
digitalWrite(INH, HIGH);  // 1
while(1)
{
digitalWrite(ADDA, LOW);  // 0
digitalWrite(ADDB, LOW);  // 0
digitalWrite(ADDC, LOW);  // 0
delay(100);
digitalWrite(ADDA, HIGH);  // 1
digitalWrite(ADDB, LOW);  // 0
digitalWrite(ADDC, LOW);  // 0
delay(100);
}
}
```

[Figure A1: Ardunio code used for controlling the multiplexer to feed signals from both control regions]

```
int INH = 6;
int ADDA = 7;
int ADDB = 12;
int ADDC = 13;

void setup() {
pinMode(ADDA, OUTPUT);
pinMode(ADDB, OUTPUT);
pinMode(ADDC, OUTPUT);
pinMode(INH, OUTPUT);
}

void loop()
{
digitalWrite(INH, HIGH);  // 1
digitalWrite(ADDA, LOW);  // 0
digitalWrite(ADDB, LOW);  // 0
digitalWrite(ADDC, LOW);  // 0
}
```

[Figure A2: Ardunio code used for controlling the multiplexer to feed a single signal from one control regions for initial testing]

Appendix B: Testing Data

				Calculated Gain	89.2
Instrumental Amplifer			Frequency fixed at 20hz	Average Gain in Range	93.9315873
volts in	Vin(p-p)	volts out	Vout expected	Instumental Amplifer Gain	
0.05	0.1	4.62	4.46	92.4	
0.045	0.09	4.16	4.014	92.44444444	
0.04	0.08	3.7	3.568	92.5	
0.035	0.07	3.24	3.122	92.57142857	
0.03	0.06	2.8	2.676	93.33333333	
0.025	0.05	2.31	2.23	92.4	
0.02	0.04	1.9	1.784	95	
0.015	0.03	1.42	1.338	94.66666667	
0.01	0.02	0.96	0.892	96	
0.005	0.01	0.49	0.446	98	

[Table B1: Testing data for the gain of the instrumental amplifier module]

Instumental amplifer and 50hz notch filter				Fixed voltage: 0.05V,	0.1Vp-p	Vout expected	4.46V
Frequency hz	Vin (V)	measured in Vin (p-p)	Vin (w/noise)	Vout(p-p)	Vout		
5	0.05	0.122	0.061	8.9200	4.46		
10	0.05	0.122	0.061	8.4000	4.2		
15	0.05	0.1065	0.05325	7.5800	3.79		
20	0.05	0.1045	0.05225	6.4990	3.2495		
25	0.05	0.97051	0.485255	5.0470	2.5235		
30	0.05	0.09158	0.04579	3.8220	1.911		
35	0.05	0.1043	0.05215	3.2380	1.619		
40	0.05	0.101	0.0505	2.1540	1.077		
45	0.05	0.1039	0.05195	1.2220	0.611		
50	0.05	0.1039	0.05195	0.3290	0.16452		
55	0.05	0.09727	0.048635	0.4622	0.2311		
60	0.05	0.101	0.0505	1.1840	0.592		
65	0.05	0.0965	0.04825	1.7680	0.884		
70	0.05	0.104	0.052	2.4900	1.245		
75	0.05	0.103	0.0515	3.0240	1.512		
80	0.05	0.1014	0.0507	3.4200	1.71		
90	0.05	0.104	0.052	4.361	2.1805		
100	0.05	0.103	0.0515	4.996	2.498		

[Table B2: Testing data for the instrumental amplifier and 50Hz notch filter modules in series]

High-Pass Filter				Fixed voltage: 1V,	2Vp-p
Frequency hz	Vin (V)	measured in Vin (p-p)	Vin (w/noise)	Vout (p-p)	Vout
5	0.25	0.5106	0.2553	0.1599	0.07995
10	0.25	0.5158	0.2579	0.2781	0.13905
15	0.25	0.5064	0.2532	0.3522	0.1761
20	0.25	0.5077	0.25385	0.4019	0.20095
25	0.25	0.5096	0.2548	0.4340	0.217
30	0.25	0.506	0.253	0.4510	0.2255
35	0.25	0.5082	0.2541	0.4652	0.2326
40	0.25	0.5072	0.2536	0.4729	0.23645
45	0.25	0.5076	0.2538	0.4811	0.24055
50	0.25	0.5094	0.2547	0.4880	0.244
55	0.25	0.507	0.2535	0.4870	0.24352
60	0.25	0.511	0.2555	0.4927	0.24635
65	0.25	0.5063	0.25315	0.4933	0.24665
70	0.25	0.5078	0.2539	0.4970	0.2485
75	0.25	0.5076	0.2538	0.4970	0.2485
80	0.25	0.5065	0.25325	0.4970	0.2485
85	0.25	0.5055	0.25275	0.4989	0.24945
90	0.25	0.507	0.2535	0.5000	0.25
95	0.25	0.5086	0.2543	0.5015	0.25075
100	0.25	0.5062	0.2531	0.5010	0.2505

[Table B3: Testing data for the 2-pole multi-feedback high-pass filter module]

Low-Pass Filter				Fixed voltage: 1V,	2Vp-p
Frequency hz	Vin (V)	measured in Vin (p-p)	Vin (w/noise)	Vout (p-p)	Vout
5	0.25	0.514	0.257	0.4920	0.246
10	0.25	0.507	0.2535	0.4372	0.2186
15	0.25	0.506	0.253	0.3807	0.19035
20	0.25	0.5049	0.25245	0.3295	0.16475
25	0.25	0.5045	0.25225	0.2862	0.1431
30	0.25	0.504	0.252	0.2510	0.1255
35	0.25	0.504	0.252	0.2250	0.1125
40	0.25	0.502	0.251	0.2010	0.1005
45	0.25	0.505	0.2525	0.1840	0.092
50	0.25	0.5	0.25	0.1640	0.082
55	0.25	0.5	0.25	0.1490	0.0745
60	0.25	0.5	0.25	0.1390	0.0695
65	0.25	0.5	0.25	0.1290	0.0645
70	0.25	0.504	0.252	0.1260	0.063
75	0.25	0.504	0.252	0.1200	0.06
80	0.25	0.504	0.252	0.1120	0.056
85	0.25	0.5003	0.25015	0.1008	0.0504
90	0.25	0.5	0.25	0.0978	0.04889
95	0.25	0.4995	0.24975	0.0912	0.04558
100	0.25	0.501	0.2505	0.0900	0.044985

[Table B4: Testing data for the 2-pole multi-feedback low-pass filter module]

Non-Inverting Amplifer				Gain average range		75.9 < G < 388.2	
Vin (V)	Vin p-p (V)	Vin w/ noise	Vin (p-p)	Vout (v)	Vout (p-p)	Gain	G = 83, R13 = 1k (ohms)
0.1	0.2	0.1021	0.2042	7.925	15.85	77.61998041	8.3
0.09	0.18	0.09325	0.1865	7.7	15.4	82.57372654	7.47
0.08	0.16	0.08315	0.1663	6.93	13.86	83.34335538	6.64
0.07	0.14	0.07375	0.1475	6.14	12.28	83.25423729	5.81
0.06	0.12	0.06375	0.1275	5.245	10.49	82.2745098	4.98
0.05	0.1	0.066	0.132	4.276	8.552	64.78787879	4.15
0.04	0.08	0.041485	0.08297	3.443	6.886	82.9938532	3.32
0.03	0.06	0.0313	0.0626	2.5305	5.061	80.84664537	2.49
0.02	0.04	0.0247	0.0494	1.83	3.66	74.08906883	1.66
0.01	0.02	0.0118	0.0236	0.56	1.12	47.45762712	0.83
Vin (mV)	Vin p-p (mV)	Vin w/ noise	Vin (p-p)	Vout (v)	Vout (p-p)	Gain	G = 455, R13 = 0k (ohms)
20	40	0.01863	0.03726	6.8850	13.77	369.5652174	9.1
18	36	0.013495	0.02699	5.2400	10.48	388.29196	8.19
16	32	0.01603	0.03206	6.3250	12.65	394.5726762	7.28
14	28	0.01329	0.02658	5.1750	10.35	389.3905192	6.37
12	24	0.011325	0.02265	4.5635	9.127	402.9580574	5.46
10	20	0.0108	0.0216	4.2900	8.58	397.2222222	4.55
8	16	0.00838	0.01676	3.3500	6.7	399.7613365	3.64
6	12	0.006385	0.01277	2.3220	4.644	363.6648395	2.73

[Table B5: Testing data for the non-inverting amplifier with adjustable gain]

50 hz notch filter				Fixed voltage: 1V,	0.1Vp-p
Frequency hz	Vin (V)	measured in Vin (p-p)	Vin (w/noise)	Vout(p-p)	Vout
5	1	2.037	1.0185	1.98	0.99
10	1	2.028	1.014	1.8720	0.936
15	1	2.038	1.019	1.7080	0.854
20	1	2.034	1.017	1.5170	0.7585
25	1	2.033	1.0165	1.3760	0.688
30	1	2.2033	1.10165	1.0530	0.5265
35	1	2.04	1.02	0.8050	0.4025
40	1	2.036	1.018	0.5712	0.2856
45	1	2.035	1.0175	0.3626	0.1813
50	1	2.028	1.014	0.1506	0.0753
55	1	2.028	1.014	0.0706	0.03531
60	1	2.027	1.0135	0.2228	0.1114
65	1	2.032	1.016	0.3767	0.18835
70	1	2.03	1.015	0.5180	0.259
75	1	2.035	1.0175	0.6382	0.3191
80	1	2.031	1.0155	0.7480	0.374
85	1	2.038	1.019	0.8556	0.42781
90	1	2.038	1.019	0.9550	0.4775
95	1	2.038	1.019	1.027	0.5135
100	1	2.024	1.012	1.09	0.545

[Table B6: Testing data for the 50Hz notch filter module]